



Run Run Shaw Library

香港城市大學
City University of Hong Kong

Copyright Warning

Use of this thesis/dissertation/project is for the purpose of private study or scholarly research only. ***Users must comply with the Copyright Ordinance.***

Anyone who consults this thesis/dissertation/project is understood to recognise that its copyright rests with its author and that no part of it may be reproduced without the author's prior written consent.

A NEW VELOCITY PROFILE
GENERATION FOR HIGH
EFFICIENCY CNC MACHINING
APPLICATION

NG YU KI

MASTER OF PHILOSOPHY

CITY UNIVERSITY OF HONG KONG

SEPTEMBER 2008

CITY UNIVERSITY OF HONG KONG

香港城市大學

A NEW VELOCITY PROFILE

GENERATION FOR HIGH EFFICIENCY

CNC MACHINING APPLICATION

用於高效率數控機床的新型速度曲線的產

生方法

Submitted to

Department of Manufacturing Engineering and Engineering

Management

製造工程及工程管理學系

by

Ng Yu Ki

吳宇基

September 2008

二零零八年九月

Abstract

Computer Numerical Control has been widely applied within the manufacturing industry due to its great productivity and relatively low cost. A challenging problem that needs to be addressed is that when increasing the motion speed to improve productivity, the CNC motion accuracy may also degrade. This thesis presents the latest effort in improving the motion planning by employing a new velocity profile to save operation time and thus enhance working efficiency, while maintaining good motion accuracy.

In traditional motion planning, S- or T-curve velocity profile is generally utilized in the design of successive movements, and the next movement starts only after the previous movement stops. In this thesis, a new velocity profile with improved S-curve is proposed, by which the next movement starts without waiting for the previous movement to stop, and thereby the operation time is saved and efficiency is improved. Two methods without jerk control and with jerk control are developed to generate this new velocity profile. The significance of the new approach lies in the reduction of machining time without degrading motion accuracy.

Experiments are finally performed in a real CNC machine application to compare the new velocity profile and the traditional velocity profile. Experimental results show that the new velocity profile without jerk control requires the shortest operation time but slightly increases of the position and contour errors when compared to the traditional velocity profile. The new velocity profile with jerk control requires less operation time and exhibits compatible motion accuracy that is an improvement against the traditional velocity profile.

Acknowledgement

I would like to give my profound thanks to my supervisor, Dr. Sun Dong, for his invaluable guidance and enduring support to me throughout the whole course of MPhil study.

I would also like to thank all colleagues in the Digital Manufacturing and Motion Control Laboratory, especially Dr. Liu Chong, for their suggestions and support to improve the work. Finally, the staff of MEEM Laboratories and the Department of MEEM provided a lot of support in the study.

Table of Contents

| | |
|---|-----|
| Abstract | i |
| Acknowledgement | ii |
| Table of Contents | iii |
| List of Figures | vi |
| List of Tables | ix |
| Chapter 1. Introduction | 1 |
| 1.1. Background | 1 |
| 1.2. Problem Statements | 2 |
| 1.3. Objectives | 3 |
| 1.4. Methodology and Significance | 3 |
| 1.5. Conclusion | 5 |
| Chapter 2. Literature Review | 6 |
| 2.1. Computer Numerical Control (CNC) Machining System | 6 |
| 2.2. Interpolation of CNC Machining | 9 |
| 2.2.1. Linear Interpolation | 10 |
| 2.2.2. Circular Interpolation | 11 |
| 2.2.3. Other Interpolations | 11 |
| 2.3. Acceleration Deceleration Before and After Interpolation | 12 |
| 2.3.1. Acceleration Deceleration After Interpolation (ADAI) | 13 |
| 2.3.2. Acceleration Deceleration Before Interpolation (ADBI) | 14 |
| 2.4. Velocity Profile | 16 |
| 2.5. Continuous Machining | 17 |

| | | |
|------------|--|----|
| 2.6. | Conclusion | 18 |
| Chapter 3. | Motion Planning with New Velocity Profile | 19 |
| 3.1. | S-curve Velocity Profile | 19 |
| 3.2. | Generation of the Typical S-curve Velocity Profile | 22 |
| 3.3. | Proposed Motion Planning with New Velocity Profile | 29 |
| Chapter 4. | Calculation of the New Velocity Profile | 32 |
| 4.1. | Motion Planning without Jerk Control..... | 32 |
| 4.1.1. | Case (i) | 32 |
| 4.1.2. | Case (ii)..... | 35 |
| 4.1.3. | Case (iii)..... | 38 |
| 4.2. | Motion Planning with Jerk Control..... | 38 |
| 4.2.1. | Case (i) | 39 |
| 4.2.2. | Case (ii)..... | 42 |
| 4.2.3. | Case (iii)..... | 44 |
| 4.3. | Simulations..... | 45 |
| 4.3.1. | Case (i) | 45 |
| 4.3.2. | Case (ii)..... | 47 |
| 4.3.3. | Case (iii)..... | 50 |
| 4.3.4. | Relationship of Time Saving and the Continuity of the Trajectory | 52 |
| Chapter 5. | Experiments | 54 |
| 5.1. | Experiments Setup | 54 |
| 5.2. | Experimental Results | 57 |
| 5.2.1. | Application of Traditional Velocity Profile..... | 58 |
| 5.2.2. | Application of New Velocity Profile without Jerk Control..... | 60 |
| 5.2.3. | Application of New Velocity Profile with Jerk Control..... | 62 |

| | |
|------------------------------|----|
| 5.3. Discussions..... | 64 |
| Chapter 6. Conclusions | 66 |
| References | 68 |

List of Figures

Chapter 2

| | |
|---|----|
| Figure 2.1 Computer Numerical Control machining system | 6 |
| Figure 2.2 Point-to-Point (PTP) system | 7 |
| Figure 2.3 Contour system | 7 |
| Figure 2.4 Open loop digital control system of a CNC machine | 8 |
| Figure 2.5 Closed loop digital control system of a CNC machine | 9 |
| Figure 2.6 Linear interpolation | 10 |
| Figure 2.7 Circular interpolation..... | 11 |
| Figure 2.8 Flowchart of Acceleration Deceleration After Interpolation | 13 |
| Figure 2.9 Control loop of Acceleration Deceleration After Interpolation | 14 |
| Figure 2.10 Flowchart of Acceleration Deceleration Before Interpolation | 15 |
| Figure 2.11 Control loop of Acceleration Deceleration Before Interpolation | 16 |
| Figure 2.12 Profiles of acceleration and deceleration..... | 16 |
| Figure 2.13 Corner error of sharp corner | 18 |

Chapter 3

| | |
|--|----|
| Figure 3.1 Traditional S-curve velocity profile..... | 20 |
| Figure 3.2 Velocity profile with (a) and without (b) segment II | 24 |
| Figure 3.3 Velocity profile without segment II | 26 |
| Figure 3.4 Velocity profile with segment II | 27 |
| Figure 3.5 Flowchart of the generation of an S-curve velocity profile..... | 29 |
| Figure 3.6 Traditional S-curve velocity profile..... | 30 |

| | |
|--|----|
| Figure 3.7 Proposed S-curve velocity profile | 31 |
| Chapter 4 | |
| Figure 4.1 New velocity profile of case (ii) | 36 |
| Figure 4.2 New velocity profile of case (iii) | 38 |
| Figure 4.3 The velocity at the end of segment V is higher than the velocity at half the time of the deceleration stage..... | 41 |
| Figure 4.4 The velocity at the end of segment V is lower than the velocity at half the time of the deceleration stage..... | 41 |
| Figure 4.5 The velocity at the end of segment I is lower than the velocity at half the time of the acceleration stage..... | 44 |
| Figure 4.6 The velocity at the end of segment I is higher than the velocity at half the time of the acceleration stage..... | 44 |
| Figure 4.7 Traditional motion planning | 46 |
| Figure 4.8 New motion planning without jerk control..... | 46 |
| Figure 4.9 New motion planning with jerk control..... | 47 |
| Figure 4.10 Traditional motion planning | 49 |
| Figure 4.11 New motion planning without jerk control..... | 49 |
| Figure 4.12 New motion planning with jerk control..... | 50 |
| Figure 4.13 Traditional motion planning | 51 |
| Figure 4.14 New motion planning without jerk control..... | 51 |
| Figure 4.15 New motion planning with jerk control..... | 52 |
| Figure 4.16 Trajectory with sharp corners | 53 |
| Figure 4.17 Trajectory without sharp corners | 53 |
| Chapter 5 | |
| Figure 5.1 Outlook of the homemade 5-axis CNC machine..... | 54 |
| Figure 5.2 Frame of the CNC machine | 55 |

| | |
|--|----|
| Figure 5.3 Motion and control system of the CNC machine | 55 |
| Figure 5.4 Machined part | 58 |
| Figure 5.5 Trajectory path in X-Y plane | 58 |
| Figure 5.6 Velocity profiles of traditional motion planning..... | 59 |
| Figure 5.7 Position errors and contour error of traditional motion planning..... | 60 |
| Figure 5.8 Velocity profiles of new motion planning without jerk control | 60 |
| Figure 5.9 Position errors and contour error of new motion planning without jerk control..... | 61 |
| Figure 5.10 Velocity profiles of new motion planning with jerk control... | 62 |
| Figure 5.11 Position errors and contour error of new motion planning with jerk control | 63 |

List of Tables

Chapter 3

| | |
|------------------------------|----|
| Table 3.1 Nomenclature | 23 |
|------------------------------|----|

Chapter 4

| | |
|---|----|
| Table 4.1 Motion specification simulation in Case (i) | 45 |
| Table 4.2 Motion specification simulation in Case (ii) | 48 |
| Table 4.3 Motion specification simulation in Case (iii) | 50 |
| Table 4.4 Motion specification | 52 |

Chapter 5

| | |
|--|----|
| Table 5.1 Specifications of the developed 5-axis machine | 56 |
| Table 5.2 Comparison of results of traditional motion planning | 59 |
| Table 5.3 Comparison of results of new motion planning without jerk control | 62 |
| Table 5.4 Comparison of results of new motion planning with jerk control | 63 |
| Table 5.5 Comparison of results | 65 |

Chapter 1. Introduction

1.1. Background

In the mid-1970s, the first Computer Numerical Control (CNC) was developed, and was displayed at a machine tool show. In the years since, the CNC rapidly developed and has become one of the most popular equipments in manufacturing industries due to its advantages of [1]: higher flexibility, increased productivity, consistent quality, and reduced manpower etc. The abilities of the CNC have dramatically increased and meanwhile the size of the control unit and cost have decreased, especially after the PC-based software-CNC system was introduced [2], [3]. Nowadays, the CNC is widely applied in metal machinery, such as mills, drills, and punch presses, but has also expanded to the applications in the metalworking of robotics and welding.

As the demands for better accuracy of complex parts and higher productivity in manufacturing industries increase, the CNC system must be developed with higher efficiency and accuracy. An important issue that affects the CNC machining application is how to balance productivity and motion accuracy. Increasing demand for greater productivity requires an increase in the motion speed in order to enhance working efficiency, but consequently the motion accuracy may degrade. Furthermore, in conventional motion planning, the frequent ramping up and ramping down at the connection of line segments highly reduce productivity.

The jerk value, which is the acceleration derivative, should be limited in order

to protect the CNC system and to maintain motion accuracy. Improper acceleration and deceleration provide sudden changes in drive forces to machine tools and cause vigorous vibrations; eventually degrading motion performance as well. Improving the efficiency of CNC machining applications without degrading motion accuracy through motion planning has been the motivation of the development of a new velocity profile generation in this study.

1.2. Problem Statements

Nowadays, a great problem encountered by manufacturers and researchers in improving the CNC technology is to achieve high accuracy and reduce the overall machining time. The most direct and simple method to enhance machining efficiency is to increase the motion speed. However, as mentioned in the previous part, motion accuracy may degrade when the motion speed increases. According to the former research works, the following three methods have been proposed to enhance the machining efficiency. The first method is multi-axis machining [4]-[7], aiming to maximize the material removal rate by maximising the point of contact and thus shortening the machining time. The second method is the tool-path planning [5]-[11], which is used to plan the maximum material removal rate path or the shortest path to enhance machining efficiency. The last method is time-optimal path planning [12]-[14], by which the optimal acceleration and velocity are selected under the physical constraints of the path.

All above methods are based on the traditional S-curve velocity profile in motion planning, in which the velocity of each movement decreases down to zero at the connection to the next movement. In this way, the operation time is wasted. There exists a clear demand for developing a new and more efficient velocity profile to “smooth” the successive movements and thus improve the machining efficiency.

In this way, the maximum velocity of each movement does not increase, and motion accuracy does not degrade. Note that fast acceleration and deceleration with high jerk requires short operation time and thus benefits working efficiency. But improper acceleration and deceleration with exceeded jerk cause vigorous vibration and degrades the motion accuracy [23]-[34].

1.3. Objectives

The objectives of this thesis work are given below.

- 1.) Propose a new methodology to shorten machining time and hence to improve CNC machining efficiency without degrading motion accuracy.
- 2.) Apply the new method to real CNC machining task to demonstrate the effectiveness of proposed method.

1.4. Methodology and Significance

- 1) Proposing a novel idea of using a new velocity profile in motion planning

In traditional motion planning, the machining tool accelerates from zero to the maximum velocity and then decelerates from the maximum velocity to zero in each movement, which causes lower productivity. To overcome this problem, an improved motion planning should be proposed for interpolation. In the new motion planning, the velocity does not decelerate to zero at the connection of two successive movements. The advances of this method are twofold. First, it can be implemented easily and effectively, without demanding for large buffer and complex facility to process huge amount of look-ahead commands. Second, it shortens the operation time via “smoothing” successive movements but not increasing the maximum velocity of each movement, and therefore does not degrade the motion accuracy.

Moreover, the proposed new velocity profile can deal with the successive machining of little line segments, in which the given maximal velocity is limited by the given short distance of each movement.

2) Developing the new velocity profile with jerk control

The new velocity profile is calculated based on modification of the S-curve velocity profile with Acceleration/ Deceleration Before Interpolation (ADBI) [35] in motion planning. The connection between the two adjacent movements will be newly designed so that the velocity does not ramp down to zero at the connection between the two movements. The new velocity profile can be generated using two methods: without jerk control and with jerk control. The difference between the two methods lies in the design of connection between the two successive movements. Without jerk control, one only considers a rapid transformation from the current movement to the next one. With jerk control, one also needs to control the jerk value within the preset maximum limit. In this way, the transaction may not be as fast as without jerk control, but the motion performance can be better guaranteed.

3) Experimental verification of the proposed velocity profile generation approach

A homemade 5-axis CNC machine setup will be established for the experimental test. The proposed new velocity profile will be applied to a real CNC machining task to verify the effectiveness of the proposed interpolator with the new motion planning methodology. The performance of the new velocity profile will be compared to that of the traditional velocity profile, in terms of both motion efficiency and accuracy.

1.5. Conclusion

This chapter discusses the research background, objectives, methodologies and significances. The focus of this research lies in proposing a new velocity profile in motion planning to improve machining efficiency without degrading motion accuracy. With the new velocity profile, the velocity does not decelerate to zero at the connection of successive movements, and thus the machining time is shortened.

The remainder of this thesis is organized as follows. Chapter 2 presents a literature review of the machining algorithm of the Computer Numerical Control (CNC), the basic types of interpolation, the acceleration deceleration motion planning architectures, and the strategy of continuous machining. Chapter 3 presents the idea of generating a new velocity profile based on S-curve in motion planning. In Chapter 4, the new motion planning with and without jerk control is developed, followed by simulation studies. Chapter 5 presents experimental verification of the proposed approaches in real CNC machining task. Finally, the conclusions of this work are given in Chapter 6.

Chapter 2. Literature Review

This chapter will present the machining system of the Computer Numerical Control (CNC), including the contouring and control systems. The basic types of interpolation of the CNC, the acceleration and deceleration motion planning architectures, and the velocity profiles and generation approach are also summarised. Finally, the strategy of continuous machining will be introduced.

2.1. Computer Numerical Control (CNC) Machining System

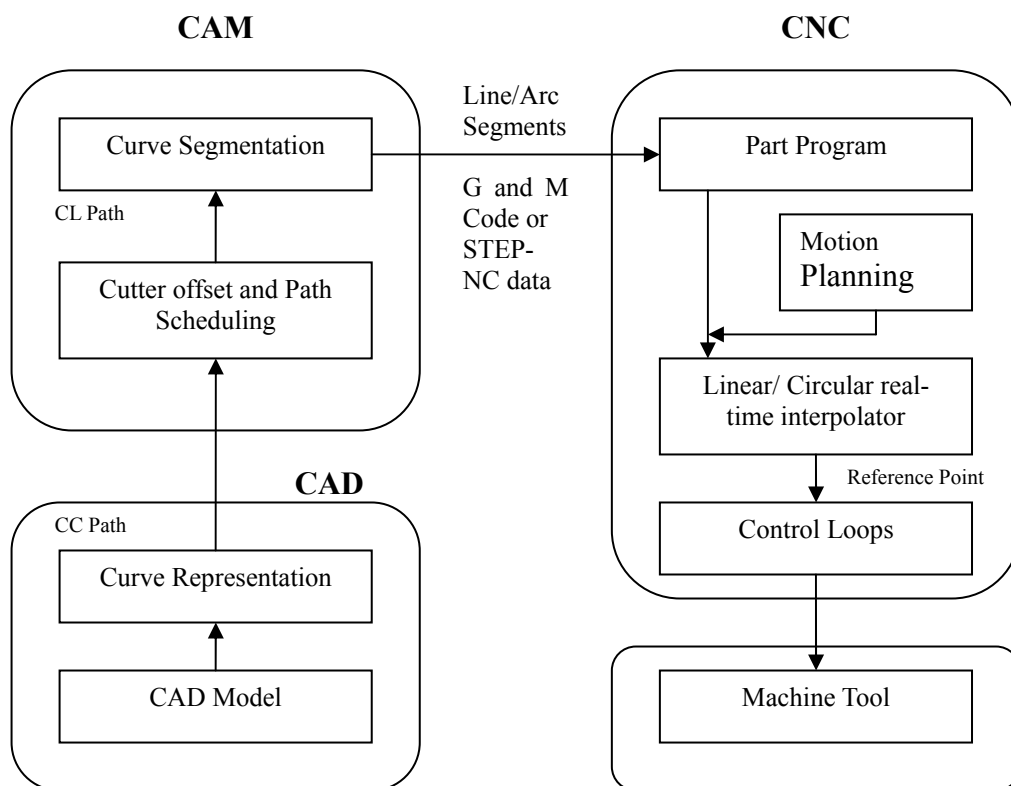


Figure 2.1 Computer Numerical Control machining system

The conventional CNC machining system is shown as Fig. 2.1 [36]. In the

manufacturing process, the part designer designs a 3D model with Computer Aided Design (CAD) software such as Solidwork, AutoCAD etc., and is represented by linear, circular, and parametric curves. The CAD system will then send the information of the curves into the Computer Aided Manufacturing (CAM) system, such that the CAM system can plan the path of the tooling with the offset of the cutter from the cutter centre to the cutter point. After the path has been decided, the curve is segmented into a linear/circular form with the G and M code (ISO 6983) [37], or STEP-NC data (ISO 14649) [38], to the CNC machine. The CNC system interpolates the segments into points in the motion planning with a linear/circular interpolator. The control command is generated for each axis to follow the path generated by the CNC system.

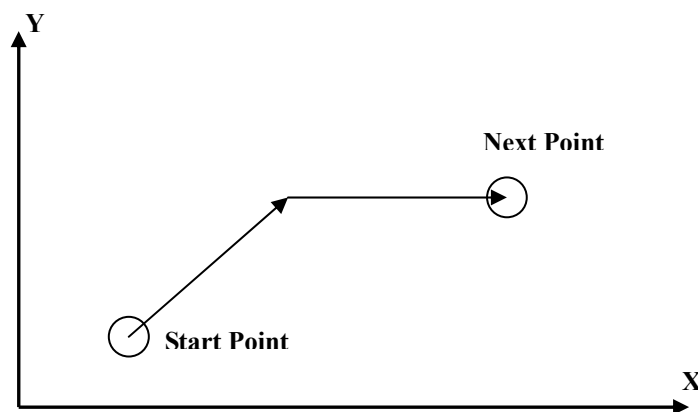


Figure 2.2 Point-to-Point (PTP) system

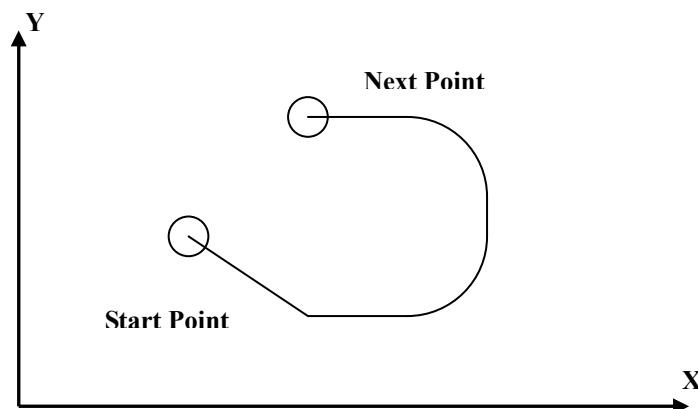


Figure 2.3 Contour system

The CNC system can be divided into two types: point-to-point (PTP) and contouring [39]. The PTP and contouring systems are shown in Figs. 2.2 and 2.3, respectively. The PTP system is widely applied in drilling machines. Koren [39] stated that, “In a PTP system, the path of the cutting tool and its feedrate while traveling from one point to the next are without any significance.” Therefore, only the position accuracy of each axis is concerned in the PTP system. For the contouring system, the cutting tools move along the workpiece while the axes of the machine are moving. The axes may move simultaneously with different velocities when the machine is contouring in a nonlinear path. Improper control of the axes would cause a contour error (defined as the distance between the closest point on the reference path and the current position) [40]. With this in mind, advanced control algorithms, such as PID control and cross-coupling technology [41], were introduced to eliminate contour error.

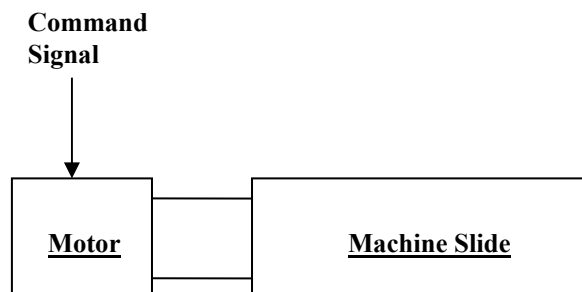


Figure 2.4 Open loop digital control system of a CNC machine

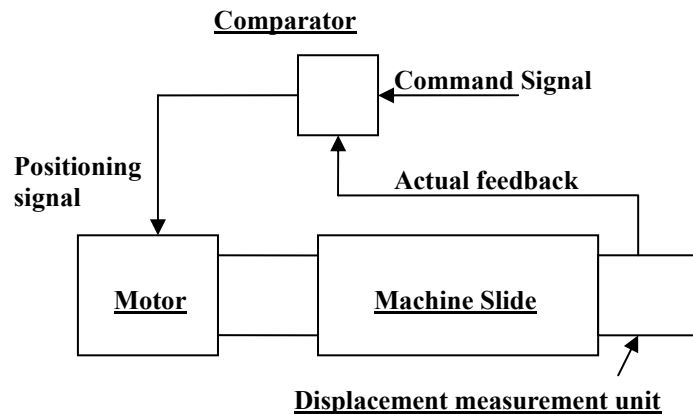


Figure 2.5 Closed loop digital control system of a CNC machine

The CNC control system can be divided into two types: an open and a closed loop control [39]. Figs. 2.4 and 2.5 show the open loop and closed loop digital control system of a CNC machine. The open loop system does not contain any feedback device, and the controller does not receive any information about the effect of the command/signals that it produces. Stepping motors are used in the open loop CNC control system. The stepping motors rotate at a fixed angle when an input pulse is applied. However, as feedback is not included in the system, the accuracy depends on the motor's ability. Therefore, the open loop control system is not common in the current CNC system. In contrast, the feedback device is included in the closed loop control system, mainly as the encoder for the positional control. The encoder is mounted at the end of the servomotors and consists of a graduated glass disc with radical gratings [1]. The increment is obtained by the disc scale through the scanning plate and photoelectric cells. Compared to the open loop control system, a close loop control system yields higher position accuracy, and thus is widely applied in the current CNC system.

2.2. Interpolation of CNC Machining

In the CNC machining system, the coordinate movement of the driven axes is

moved separately to generate the required path. By specifying the coordinates of the end-point and the centre (for a circular interpolator), the command path is generated by the interpolator. The process that produces the required shape based on the input parameters is interpolation, and the unit that generates the reference signal is the interpolator. The machining path is generated from the combination of two basic types of interpolator: linear and circular.

2.2.1. Linear Interpolation

Linear interpolation is termed as the method that produces command points connected by a straight line between the initial and final coordinates. Linear interpolation can produce the straight line in 2-D by driving one or two axes, or in space 3-D with three axes. Moreover, the rotary motions can be performed with the rotary axes. Fig. 2.6 shows the linear interpolation.

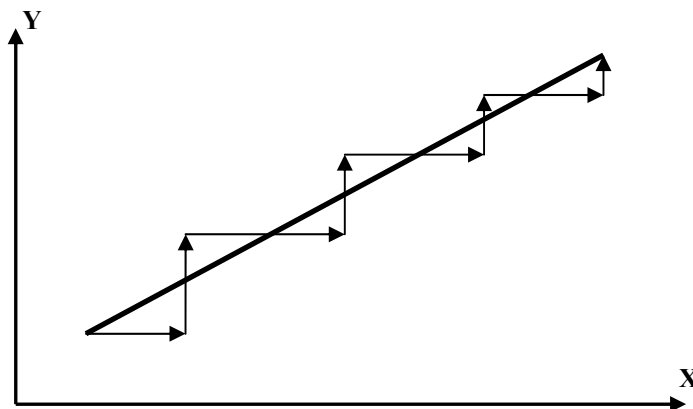


Figure 2.6 Linear interpolation

2.2.2. Circular Interpolation

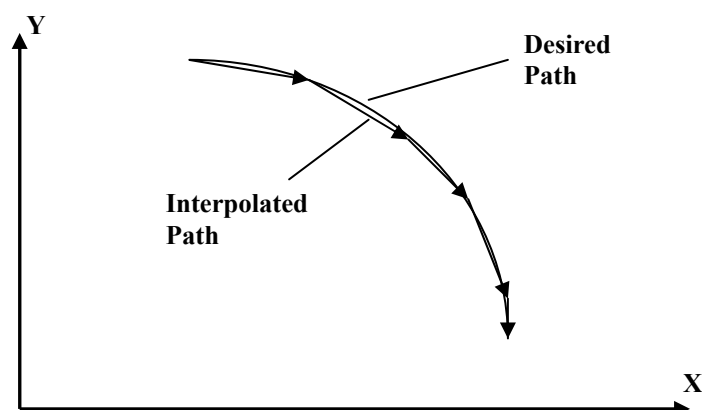


Figure 2.7 Circular interpolation

Interpolation of a circular motion has become a standard feature in the CNC machine nowadays. In a typical circular interpolation, only the initial point, final point, and the centre are required to generate the arc or circle. The circular interpolation is shown in Fig. 2.7. The radius is calculated by the machine control units, and the arc or circle is performed. The simultaneous motion of two axes at a constant tangential velocity generates a circular arc. The axial velocity of the X- and Y- axes are

$$V_x(t) = V \sin \theta(t) \quad (2.1)$$

$$V_y(t) = V \cos \theta(t) \quad (2.2)$$

2.2.3. Other Interpolations

In addition to linear and circular interpolation, other kinds of interpolation have been proposed in past researches. Parabolic interpolation [42] was proposed for the manufacturing of free-form shapes in the automotive industry in the past. Helical interpolation [42] allows single or multi-start threads to be performed on the work piece. Shpitalni et al. also proposed a parametric interpolator [35] for free-form

interpolation. Later on, many researches were carried out for parametric interpolation [43]–[47]. Unlike linear and circular interpolators, the parametric interpolator requires a high level of computation power, and kinematic constraints are taken into account for the shape of the parametric curve. Thus, attention has been drawn to the speed control algorithm [48]–[50] of parametric interpolation in recent years.

2.3. Acceleration Deceleration Before and After Interpolation

Generally, there are two types of acceleration deceleration motion planning architectures [51]: Acceleration Deceleration After Interpolation (ADAI), and Acceleration Deceleration Before Interpolation (ADBI). The difference between ADAI and ADBI will be described in the coming paragraph.

2.3.1. Acceleration Deceleration After Interpolation (ADAI)

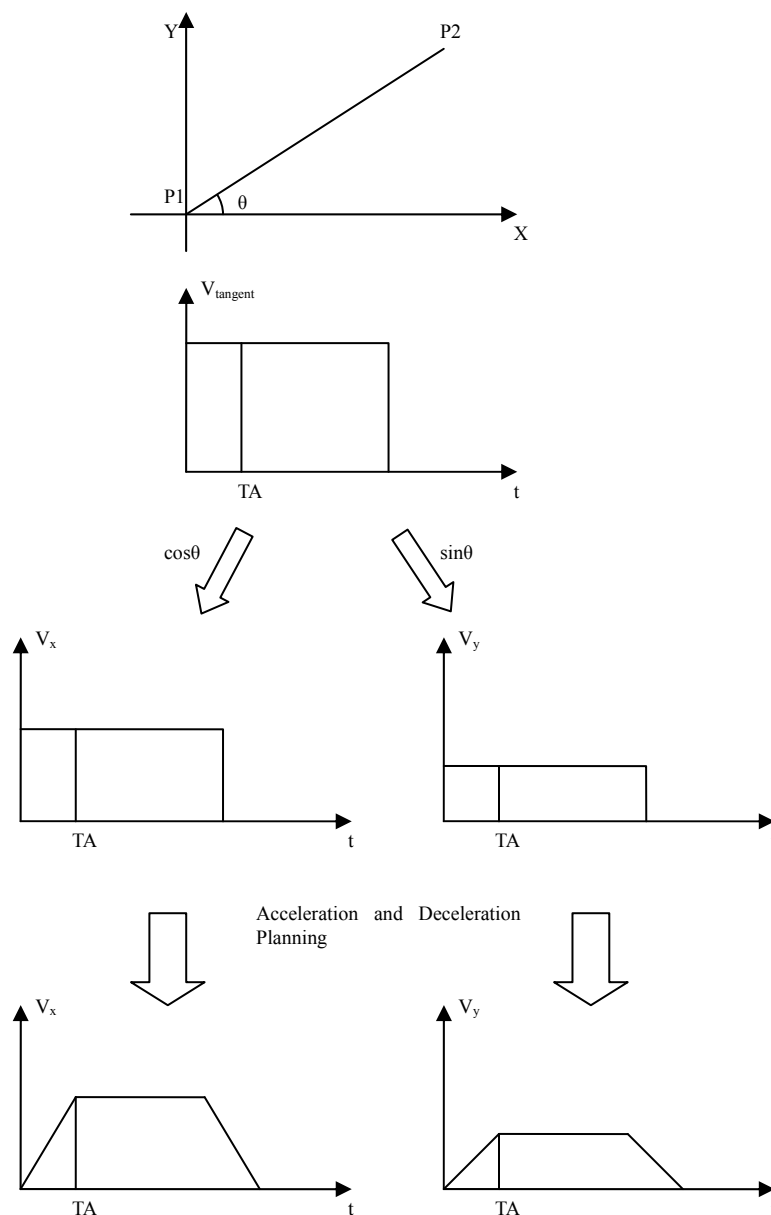


Figure 2.8 Flowchart of Acceleration Deceleration After Interpolation

Acceleration Deceleration After Interpolation (ADAI) is used to calculate the interpolation points of the axes without considering acceleration and deceleration. The interpolation command is sent to the acceleration/deceleration apparatus of each axis. The flowchart and the control loop of ADAI are shown in Figs. 2.8 and 2.9,

respectively. ADAI is widely used in conventional CNC machines because of its simple implementation.

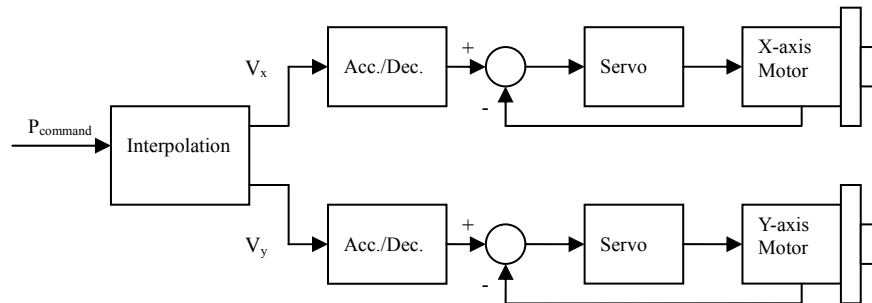


Figure 2.9 Control loop of Acceleration Deceleration After Interpolation

2.3.2. Acceleration Deceleration Before Interpolation (ADBI)

The flowchart and control loop of Acceleration Deceleration Before Interpolation (ADBI) are shown in Figs. 2.10 and 2.11, respectively. ADBI is used to calculate the acceleration and deceleration of the tangent direction before calculating the interpolation position of each axis. The interpolation command is then sent to the control unit of each axis. Although ADAI is simply implemented in the CNC machine, the better machining accuracy of ADBI is obtained when no path command error occurs in ADBI, but not ADAI [52]. In this thesis, ADBI will be employed.

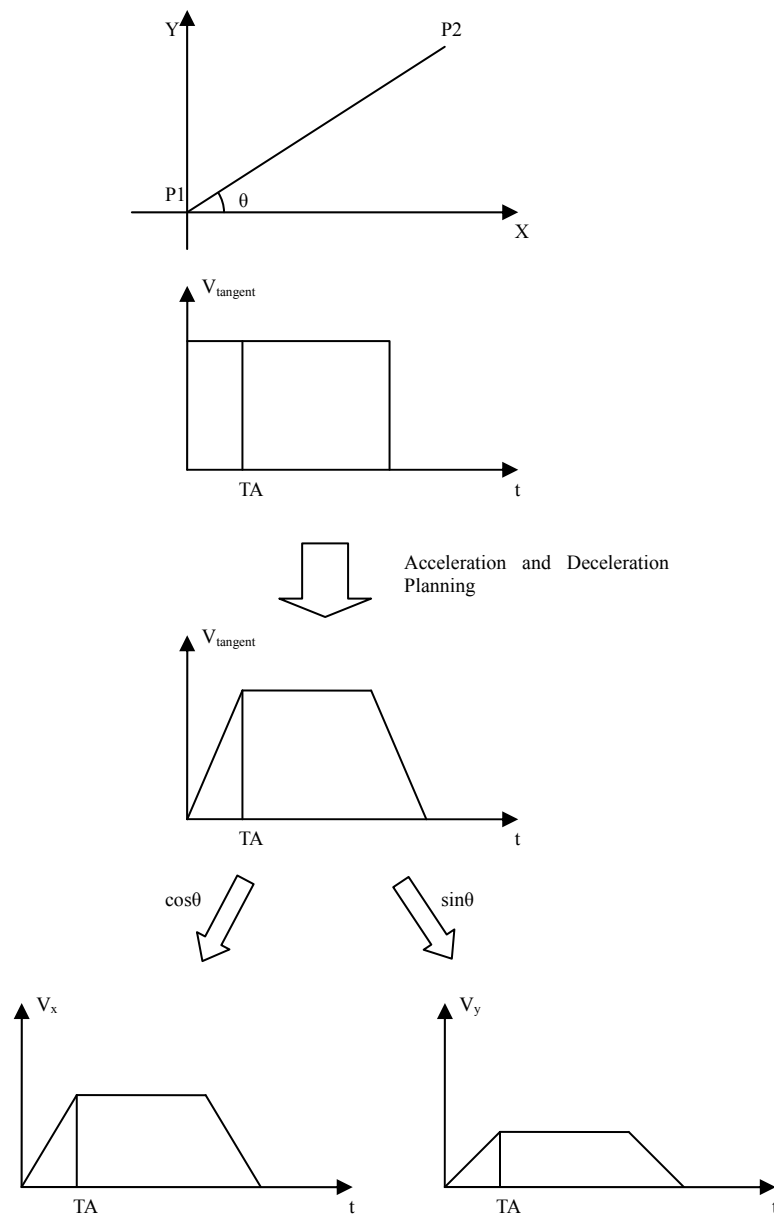


Figure 2.10 Flowchart of Acceleration Deceleration Before Interpolation

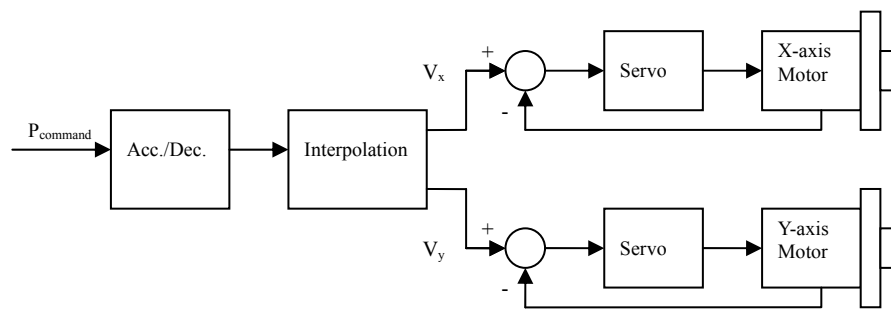


Figure 2.11 Control loop of Acceleration Deceleration Before Interpolation

2.4. Velocity Profile

In conventional CNC machines, there are three types of acceleration and deceleration velocity profiles: a) trapezoidal, b) exponential, and c) S-curve. The velocity profiles are shown in Fig. 2.12 [53]. Kim et al. [52], [54] compared the velocity profiles as mentioned before, and concluded that the machining performance of an S-curve velocity profile is the best, and the exponential velocity profile is the worst. In accounting for machining accuracy and the complexity of implementation, the S-curve velocity profile is employed in this thesis.

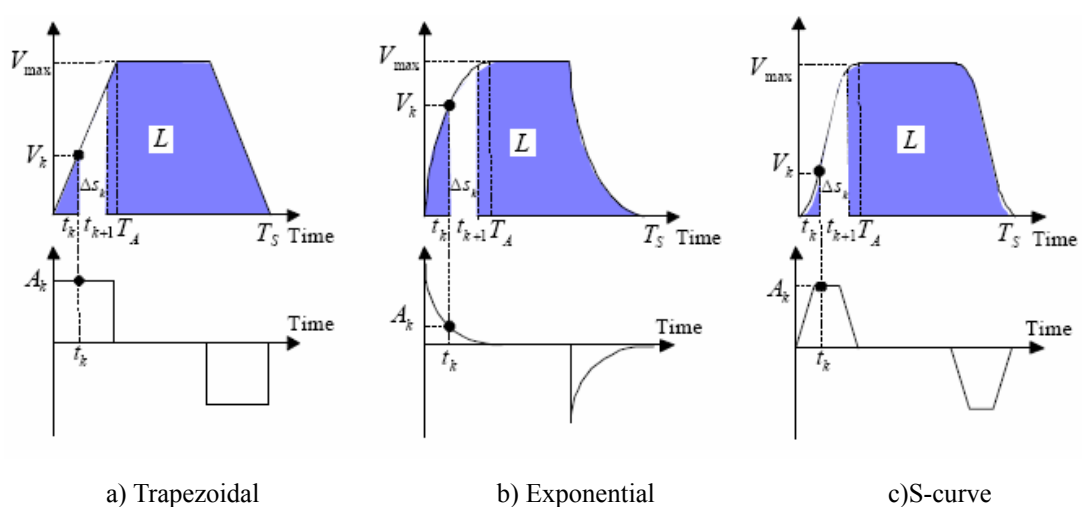


Figure 2.12 Profiles of acceleration and deceleration

Generally, there are two types of technique to generate the velocity profile. One is based on digital convolution [39], [55], which is easily implemented by the

hardware. With this method, the gradient of deceleration and acceleration must be the same when generating the velocity profile. The other is based on the selection of polynomial [56]. By employing this method, the velocity profile can be changed easily at software level, and the deceleration of velocity is independent of acceleration.

2.5. Continuous Machining

In previous research, Lam [21] proposed a new velocity profile generation approach to enhance the efficiency of successive trajectory motions by continuously machining, but the jerk was not limited in his method. As mentioned before, when an excess jerk value occurs with machining tools, it damages the machine and causes excess vibrations during the machining process. Therefore, a jerk-limited velocity profile generation approach is proposed in this thesis for continuous machining.

In the commercial arena, the look-ahead scheme [22] is applied by some well-known CNC machine manufactures, such as SIEMENS [18] and FANUC [19], for enhancing machining efficiency small line segments. Small line segment is defined as those segments where the resultant maximum velocity does not achieve the maximum velocity. However, the core algorithms of the look-ahead scheme are still kept secret, as they are commercially sensitive. Moreover, the look-ahead scheme demands large buffer and high computation power to process huge amount of look-ahead commands.

Furthermore, the automatic corner deceleration function is also applied to enhance the efficiency at the sharp corners [15]-[17], [20]. This method would degrade the machining accuracy at the sharp corners when compared to the traditional method. Fig. 2.13 [17] illustrates the strategy of automatic corner

deceleration. When the function of automatic corner deceleration is applied, the planning of allowable corner velocity is calculated from the corner angle and the maximum allowable corner error. The velocity is automatically overridden at the connection point of two movements. The corner error, denoted ε , is calculated by Eq (2.3), where ε_{max} is the maximum allowable corner error expressed as

$$\varepsilon = \frac{\sqrt{2 - 2 \cos \theta}}{\sin \theta} \cdot \varepsilon_{max} \quad (2.3)$$

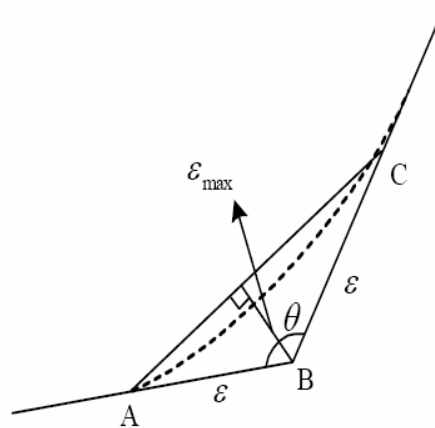


Figure 2.13 Corner error of sharp corner

2.6. Conclusion

This chapter reviews the literature works of the Computer Numerical Control (CNC) technology. Researches on interpolation of the CNC, acceleration and deceleration motion planning architectures, velocity profiles and generation approach, and continuous machining are summarised. In this thesis work, the ADBI and S-curve velocity profile will be adopted, and the velocity profile will be generated based on the polynomial selection. The linear and circular interpolations will be applied in the experiment.

Chapter 3. Motion Planning with New Velocity Profile

In traditional motion planning, the S-curve velocity profile is generally utilized in the design of successive movements, and the next movement starts only after the current movement stops. However, frequent velocity change causes poor machining efficiency. In this chapter, a new velocity profile with an improved S-curve is proposed for motion planning, by which the next movement starts without waiting for the previous movement to stop.

3.1. S-curve Velocity Profile

A traditional velocity profile can be divided into seven segments, as shown in Fig. 3.1 Segment I is defined as the region within the time period from 0 to T_1 , segment II is defined as the time period from T_1 to T_2 , and segments III, IV, V, VI, and VII are defined similarly.

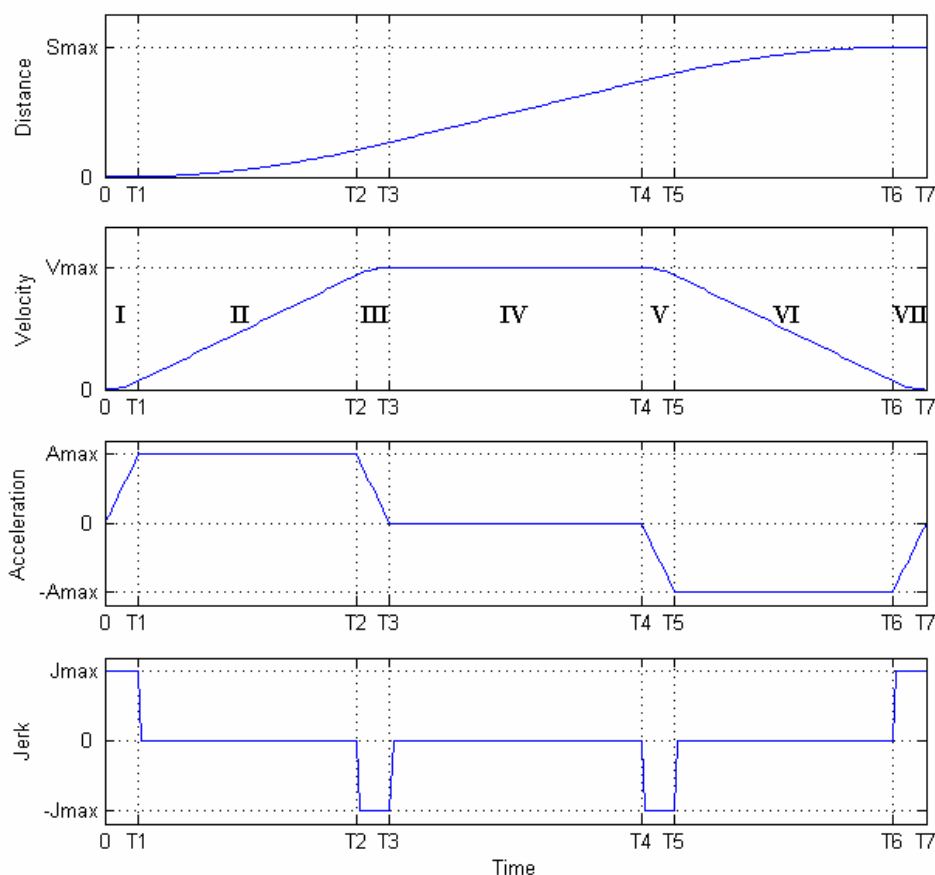


Figure 3.1 Traditional S-curve velocity profile

The area from time 0 to T_3 , is called the acceleration area (ramp up). In this area, velocity is raised from zero to the maximum of the movement. The maximum acceleration is reached in segment II, and the jerk is zero in this segment. The maximum jerk and the maximum negative jerk occur in segments I and III, respectively. Acceleration is raised from zero to the maximum and descends from maximum to zero in segments I and III, respectively.

The area from time T_3 to T_4 is the constant velocity profile (cruise). In this area, movement is at the maximum velocity, while acceleration and jerk are zero.

The area from time T_5 to T_7 , is the deceleration area (ramp down). In this area, velocity descends from the maximum of the movement to zero. Maximum deceleration is reached in segment VI, and the jerk is zero in this segment. The maximum negative jerk and the maximum jerk occur in segments V and VII,

respectively. Deceleration is raised from zero to maximum and it descends from maximum to zero in segments V and VII, respectively.

Consider Fig. 3.1, the formulae of the distance, velocity, acceleration, and jerk at i th ($i = 1, 2, \dots, 7$) segment are shown below [30].

The jerk profile of a traditional S-curve can be written as

$$J(t) = \begin{cases} J_{\max} & 0 \leq t < T_1 \\ 0 & T_1 \leq t < T_2 \\ -J_{\max} & T_2 \leq t < T_3 \\ 0 & T_3 \leq t < T_4 \\ -J_{\max} & T_4 \leq t < T_5 \\ 0 & T_5 \leq t < T_6 \\ J_{\max} & T_6 \leq t < T_7 \end{cases} \quad (3.1)$$

The acceleration profile of a traditional S-curve can be written as

$$A(t) = \begin{cases} J_{\max} t, & 0 \leq t < T_1 \\ A_{\max} & T_1 \leq t < T_2 \\ -J_{\max} (t - T_2) + A_{\max} & T_2 \leq t < T_3 \\ 0 & T_3 \leq t < T_4 \\ -J_{\max} (t - T_4) & T_4 \leq t < T_5 \\ -A_{\max} & T_5 \leq t < T_6 \\ J_{\max} (t - T_6) - A_{\max} & T_6 \leq t < T_7 \end{cases} \quad (3.2)$$

The velocity profile of a traditional S-curve can be written as

$$V(t) = \begin{cases} \frac{1}{2}J_{\max}t^2 + V_s & 0 \leq t < T_1 & V_s : \text{initial feedrate} \\ A_{\max}(t-T_1) + V_1 & T_1 \leq t < T_2 & V_1 = \frac{1}{2}J_{\max}T_1^2 + V_s \\ A_{\max}(t-T_2) - \frac{1}{2}J_{\max}(t-T_2)^2 + V_2 & T_2 \leq t < T_3 & V_2 = A_{\max}(T_2-T_1) + V_1 \\ V_3 & T_3 \leq t < T_4 & V_3 = A_{\max}(T_3-T_2) - \frac{1}{2}J_{\max}(T_3-T_2)^2 + V_2 \\ -\frac{1}{2}J_{\max}(t-T_4)^2 + V_4 & T_4 \leq t < T_5 & V_4 = V_3 \\ -A_{\max}(t-T_5) + V_5 & T_5 \leq t < T_6 & V_5 = -\frac{1}{2}J_{\max}(T_5-T_4)^2 + V_4 \\ -A_{\max}(t-T_6) + \frac{1}{2}J_{\max}(t-T_6)^2 + V_6 & T_6 \leq t < T_7 & V_6 = -A_{\max}(T_6-T_5) + V_5 \end{cases} \quad (3.3)$$

The distance traveled in each segment S-curve can be written as

$$S(t) = \begin{cases} \frac{1}{6}J_{\max}t^3 + V_s t & 0 \leq t < T_1 \\ \frac{1}{2}A_{\max}(t-T_1)^2 + V_1(t-T_1) & T_1 \leq t < T_2 \\ \frac{1}{2}A_{\max}(t-T_2)^2 - \frac{1}{6}J_{\max}(t-T_2)^3 + V_2(t-T_2) & T_2 \leq t < T_3 \\ V_3(t-T_3) & T_3 \leq t < T_4 \\ -\frac{1}{6}J_{\max}(t-T_4)^3 + V_4(t-T_4) & T_4 \leq t < T_5 \\ -\frac{1}{2}A_{\max}(t-T_5)^2 + V_5(t-T_5) & T_5 \leq t < T_6 \\ -\frac{1}{2}A_{\max}(t-T_6)^2 + \frac{1}{6}J_{\max}(t-T_6)^3 + V_6(t-T_6) & T_6 \leq t < T_7 \end{cases} \quad (3.4)$$

3.2. Generation of the Typical S-curve Velocity Profile

A general method to generate an S-curve velocity profile will be given below. Unlike the method proposed by Erkorkmaz and Altintas [30], this method requires the input of the total length, the maximum jerk, the maximum acceleration, and the maximum velocity, while the initial and final velocity is not required.

The maximum velocity of the present curve is determined by the following equations in this section.

Table 3.1 Nomenclature

| Symbol | Definition |
|---------------|--|
| J_{max} | Maximum jerk |
| J_D | New jerk of deceleration |
| J_A | New jerk of acceleration |
| A_{max} | Maximum deceleration |
| ΔV_i | Velocity change of ith segment ($i = 1\sim 7$) |
| V_f | Resultant velocity at the connection point |
| V_s | Initial velocity |
| V_i | Velocity at the end of ith segment ($i = 1\sim 7$) |
| V_{i_pro} | Proposed final velocity of ith segment ($i = 1\sim 7$) |
| V_{D_half} | Resultant velocity at the half time of the deceleration stage |
| V_{A_half} | Resultant velocity at the half time of the acceleration stage |
| S_i | Original displacement of ith segment ($i = 1\sim 7$) |
| S_{i_new} | New displacement of ith segment ($i = 1\sim 7$) |
| S_{rem} | Displacement of the original deceleration stage |
| $S_{total-i}$ | Displacement of ith movement ($i = 1\sim 2$) |
| t_D | Time spent from the maximum velocity decelerated to resultant velocity at the connection point |
| t_A | Time spent from the resultant velocity accelerated to maximum velocity at the connection point |
| t_d | Half deceleration time of new velocity profile |
| t_a | Half acceleration time of new velocity profile |
| T_i | Time at the end of the original ith segment ($i = 1\sim 7$) |
| T_{i_new} | New time of the original ith segment ($i = 1\sim 7$) |
| t_i | Time interval of new ith segment ($i = 1\sim 7$) |
| t_{i_temp} | Temporary time of ith segment ($i = 1\sim 7$) |

First, it is assumed that the acceleration of segment I achieves the maximum acceleration. By Eq (3.2), the acceleration of the segment I is

$$A_1 = A_{max} = J_{max} t_{1_temp} \quad (3.5)$$

Rewrite Eq (3.5) to yield t_{1_temp} as

$$t_{1_temp} = \frac{A_{max}}{J_{max}} \quad (3.6)$$

The velocity at the end of segment I is

$$V_1 = \frac{J_{\max} t_{1_temp}^2}{2} \quad (3.7)$$

When the time intervals of segment I and segment III are the same, the velocity changes of the two segments are the same.

In the conventional S-curve velocity profile, there are two stages of acceleration: with and without segment II. Figs. 3.2 (a) and (b) illustrate these two cases.

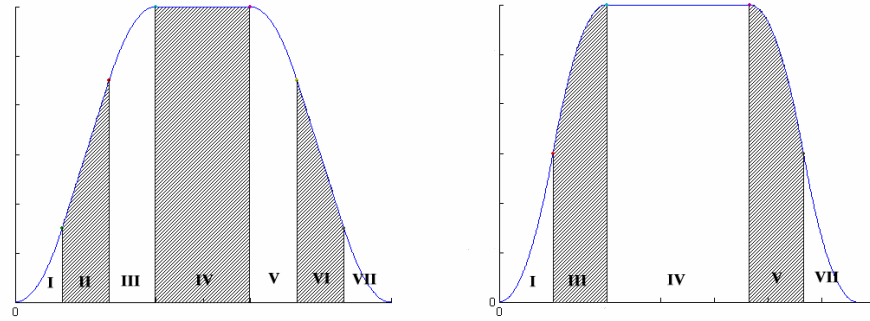


Figure 3.2 Velocity profile with (a) and without (b) segment II

Which case to be used depends on whether V_1 is greater than half of the maximum velocity. If V_1 is greater than half the maximum velocity, segment II is absent, and the maximum acceleration cannot be achieved. Otherwise, segment II is present, and the maximum acceleration can be achieved.

In the case that $V_1 < 0.5V_{\max}$, it can be assumed that the velocity at the end of segment III, denoted V_3 , is the maximum velocity in the curve at the moment. The velocity at the end of segment II is

$$V_2 = V_{\max} - \Delta V_3 = V_{\max} - V_1 \quad (3.8)$$

The velocity of segment II can be obtained by

$$V_2 = V_1 + A_1(t_{2_temp}) \quad (3.9)$$

Combining Eq (3.8) and (3.9), the time intervals of segments II and III are

$$t_{2_temp} = \frac{V_{\max} - 2V_1}{A_2} \quad (3.10)$$

$$t_{3_temp} = t_{1_temp} \quad (3.11)$$

In the case that $V_1 \geq 0.5V_{\max}$, segment II is eliminated. The maximum velocity in this case is assumed at the end of segment III

$$V_{\max} = V_3 = V_1 + \Delta V_3 = 2V_1 \quad (3.12)$$

Rewrite Eq (3.12) with Eq (3.7), the time interval of segment I is:

$$t_{1_temp} = \sqrt{\frac{V_{\max}}{J_{\max}}} \quad (3.13)$$

The spent times by segment II and segment III are

$$t_{2_temp} = 0 \quad (3.14)$$

$$t_{3_temp} = t_{1_temp} \quad (3.15)$$

Note that the time interval depends on not only the maximum velocity but also the displacement of the movement. The time intervals of the segments obtained above must also meet the requirements of the total displacement. If the displacement from segments I to III is more than half of the total displacement, the time intervals of segments I, II, and III should be decreased. To meet this displacement requirement, segment II may be shortened or removed. If $S_1 + S_3 > 0.5S$, segment II is ignored. Fig. 3.3 illustrates the velocity profile of segments I to III.

The $S_1 + S_3$ is obtained by

$$S_1 + S_3 = 2V_1 t_{1_temp} \quad (3.16)$$

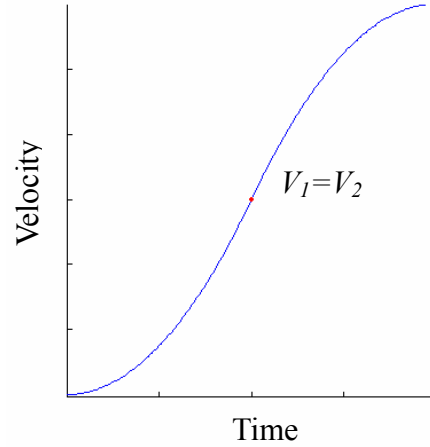


Figure 3.3 Velocity profile without segment II

The velocity of the first half of the velocity profile is

$$t_{1_temp} V_3 = 0.5S \quad (3.17)$$

where S is the total displacement. Substituting Eq (3.7) into (3.17), the new time spent in segments I, II, and III is

$$t_{1_temp} = \sqrt[3]{\frac{0.5S}{J_{\max}}} \quad (3.18)$$

$$t_{2_temp} = 0 \quad (3.19)$$

$$t_{3_temp} = t_{1_temp} \quad (3.20)$$

If $S_1 + S_3 \leq 0.5S$, the time interval of segment II is shortened so that the following requirements can be achieved. Fig. 3.4 illustrates the velocity profile from segment I to III with segment II.

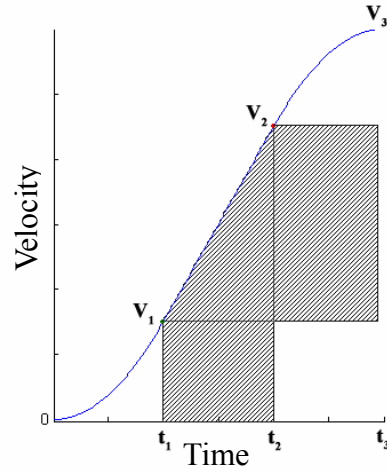


Figure 3.4 Velocity profile with segment II

The summation of the bright area and the shaded area is equal to half the total displacement. The total area is

$$0.5S = 2V_1 t_{1_temp} + S_2 + (t_{3_temp})(V_2 - V_1) \quad (3.21)$$

The displacement of segment II is

$$S_2 = (t_{2_temp}) \left(\frac{A_2(t_{2_temp})}{2} + V_1 \right) \quad (3.22)$$

The velocity of segment II is

$$V_2 = A_2(t_{2_temp}) + V_1 \quad (3.23)$$

Substituting Eqs (3.5), (3.22), and (3.23) into (3.21), and $t_{3_temp} = t_{1_temp}$ yields

$$J_{\max} t_{1_temp} (t_{2_temp})^2 + 3J_{\max} t_{1_temp}^2 (t_{2_temp}) + 2J_{\max} t_{1_temp}^3 - S = 0 \quad (3.24)$$

Solving Eq (3.25) with a quadratic formula, the time spent of segment II is

$$t_{2_temp} = \frac{1}{2J_{\max} t_{1_temp}} \left(-3J_{\max} t_{1_temp}^2 + \sqrt{J_{\max}^2 t_{1_temp}^4 + 4J_{\max} t_{1_temp} S} \right) \quad (3.25)$$

The time intervals t_{1_temp} and t_{3_temp} remain unchanged. The time intervals t_1 , t_2 , and t_3 are

$$t_1 = t_{1_temp} \quad (3.26)$$

$$t_2 = t_{2_temp} \quad (3.27)$$

$$t_3 = t_{3_temp} \quad (3.28)$$

Finally, t_4 is obtained by

$$t_4 = \frac{S - 2(S_1 + S_2 + S_3)}{V_3} \quad (3.29)$$

and t_5 , t_6 , and t_7 are expressed by

$$t_5 = t_1 \quad (3.30)$$

$$t_6 = t_2 \quad (3.31)$$

$$t_7 = t_1 \quad (3.32)$$

The flowchart of the generation of a typical S-curve velocity profile is shown in Fig.

3.5.

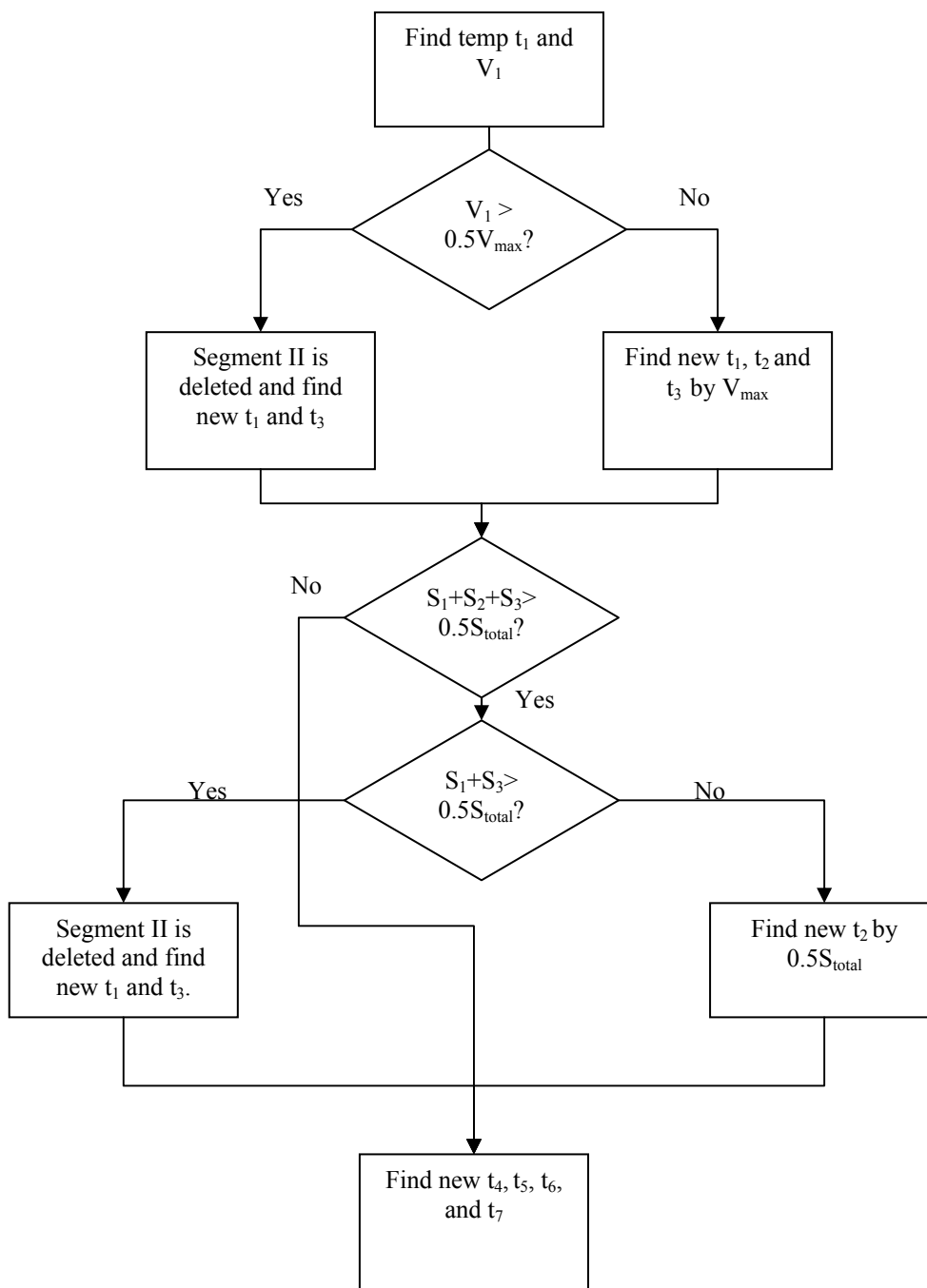


Figure 3.5 Flowchart of the generation of an S-curve velocity profile

3.3. Proposed Motion Planning with New Velocity Profile

In a traditional S-curve velocity profile with successive movements, the new movement starts only after the velocity of the current movement decreases to zero, as seen in Fig. 3.6. Since the next movement cannot start until the previous one

completely stops, considerable operation time is wasted, especially when huge numbers of successive movements are involved. In this paper, we propose a new velocity profile with an improved S-curve trajectory, as seen in Fig. 3.7. With this new velocity profile, the velocity does not decrease to zero at the connection of movements, and hence operation time is saved. The final velocity of the current movement is determined by the maximum velocity of the next movement. The new velocity profile can be generated with two different methods. One is with jerk control and the other is without jerk control [21]. The method without jerk control may exceed the preset maximum jerk value during the machining process. The method with jerk control can control the jerk within the limited maximum jerk.

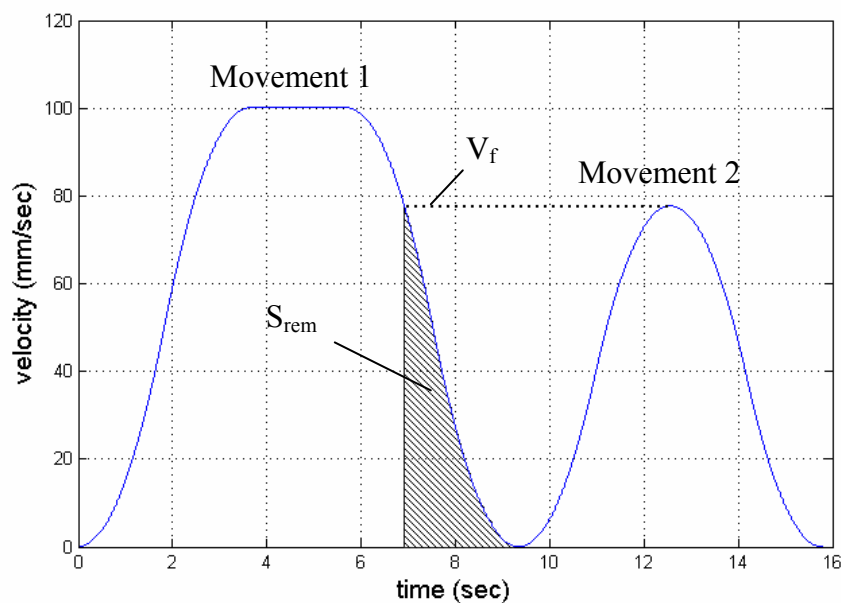


Figure 3.6 Traditional S-curve velocity profile

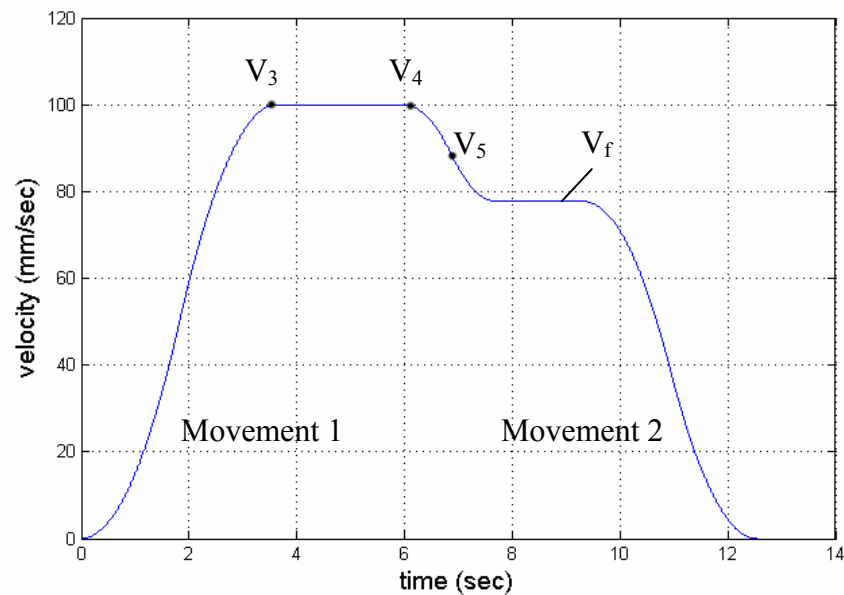


Figure 3.7 Proposed S-curve velocity profile

The key to such a new velocity profile design lies in a proper connection between the two adjacent movements. To ensure that the moving distance remains unchanged when using the new velocity profile, the area under the new velocity curve must remain unchanged. The design methodology will be detailed in the next chapter.

Note that the proposed new velocity profile suits to the tangent case where the continuous machining path is considered only. The method does not suit to the machining at the corner angle section, where the connection of the two movements is not continuous and the velocity must be zero at the connecting point.

The methodology of acceleration/deceleration before interpolation [51] is used to calculate the acceleration and deceleration along the tangent direction of the motion. The interpolation positions are then provided to the control units that drive the axes. In this study, acceleration/deceleration before interpolation will be incorporated into the new velocity profile.

Chapter 4. Calculation of the New Velocity Profile

In the previous chapter, the new motion planning methodology was introduced. The velocity does not decrease to zero at the connection of movements. In this chapter, calculation of the new velocity profile, without and with jerk control, will be proposed. Three cases will be investigated: (i) maximum velocity of the first movement is higher than that of the second movement; (ii) maximum velocity of the first movement is lower than that of the second movement; and (iii) maximum velocities of the two movements are the same. Simulations will be performed to demonstrate the effectiveness of the new velocity profiles with and without jerk control, respectively.

4.1. Motion Planning without Jerk Control

A motion planning without jerk control [21] is introduced first, and the symbols of the equations are defined in Table 3.1. Define the maximum velocity of the first movement as V_A , and the maximum velocity of the second movement as V_B . When V_A is greater, the final velocity is V_B , and when V_B is greater, the final velocity is V_A . In some cases, V_A is the same as V_B ; either V_A or V_B is the final velocity.

4.1.1. Case (i)

In this case, the maximum velocity of the first movement is higher than that of

the second movement as shown in Fig. 3.7.

1) *Velocity profile of the first movement*

For the first movement (see Fig. 3.6) to realize the new velocity profile as shown in Fig. 3.7, segment VI (see Fig. 3.1) should be eliminated. The time spent from velocity at the start of segment, to the final velocity of the movement in the new velocity profile, denoted by V_f (see Fig. 3.7), can be determined as

$$t_D = \begin{cases} \sqrt{\frac{-2(V_f - V_4)}{J_{\max}}} & V_4 > V_f \geq V_5 \\ \frac{(V_5 - V_f)}{A_{\max}} & V_5 > V_f \geq V_6 \\ t_7 - \sqrt{\frac{2V_f}{J_{\max}}} & V_6 > V_f \geq V_7 \end{cases} \quad (4.1)$$

Note that V_f is determined based on the maximum velocity of the second movement in this case. The final velocity is defined as the velocity that is shared by two successive movements at the connection area. The maximum acceleration A_{\max} is used in Eq (4.1) (as well as the following calculations) to ensure that the acquired acceleration stays within its preset value. The area below the final velocity V_f , in the deceleration stage of the original velocity profile (see Fig. 3.6), is

$$S_{rem} = \begin{cases} S_1 + S_2 + S_3 - \left(-\frac{1}{6} J t_D^3 + V_4 t_D \right) & V_4 > V_f \geq V_5 \\ S_1 + S_2 - \left(V_5 t_D - \frac{1}{2} A_{\max} t_D^2 \right) & V_5 > V_f \geq V_6 \\ S_1 - \left(-\frac{1}{2} A_{\max} t_D^2 + \frac{1}{6} J_{\max} t_D^3 + V_6 t_D \right) & V_6 > V_f \geq V_7 \end{cases} \quad (4.2)$$

To smoothly transfer velocity from the first movement to the second movement, the ramping down area of segments V to VII must be revised. Define t_d as the half

deceleration time from V_4 to V_f . Since segment VI is eliminated and $t_6 = 0$, we can design the time intervals of segments V and VII as:

$$t_5 = t_7 = t_d \quad (4.3)$$

Then t_d is calculated by

$$t_d = \frac{(S_1 + S_2 + S_3 - S_{rem})/2}{(V_f + V_4)/2} \quad (4.4)$$

Note that $V_3 = V_4$ in Eq (4.4). Define J as the jerk in the deceleration. We then have the following equation

$$\frac{(V_4 - V_f)}{2} = \int_0^{t_d} J dt \quad (4.5)$$

From Eq (4.5), the jerk can be calculated by:

$$J_D = \frac{(V_3 - V_f)}{t_d^2} \quad (4.6)$$

The time intervals of segments V, VI, and VII are

$$t_5 = t_d; t_6 = 0; t_7 = t_5 \quad (4.7)$$

Further, the time interval of segment IV is modified to ensure that the total moving distance of the first movement, denoted by $S_{total-1}$, remains unchanged. The time interval of segment IV is

$$t_4 = \frac{S_{total-1} - (S_1 + S_2 + S_3 + S_{5_new} + S_{7_new})}{V_4} \quad (4.8)$$

The resultant time of seven segments of the first movement is

$$\begin{aligned} T_{1_new} &= T_1 \\ T_{2_new} &= T_2 \\ T_{3_new} &= T_3 \\ T_{4_new} &= T_3 + t_4 \\ T_{5_new} &= T_{4_new} + t_5 \\ T_{6_new} &= T_{5_new} + t_6 \\ T_{7_new} &= T_{6_new} + t_7 \end{aligned} \quad (4.9)$$

2) Velocity of the second movement

The maximum velocity of the second movement is the same as the final velocity of the first movement. The acceleration stage of the second movement does not exist, and the velocity profile is modified by deleting segments I, II, and III. Therefore, the time intervals of segments I, II, and III are all zero, i.e.,

$$t_1 = 0; t_2 = 0; t_3 = 0 \quad (4.10)$$

With the new time intervals derived above, the area under the new velocity profile becomes smaller. To ensure that the moving distances under the existing and new velocity profiles are the same, the area difference between the two velocity profiles must be compensated by extending segment IV. The new time interval of segment IV after compensation is

$$t_4 = \frac{S_{total-2} - (S_5 + S_6 + S_7)}{V_4} \quad (4.11)$$

The resultant time of seven segments of the first movement is

$$\begin{aligned} T_{1_new} &= t_1 \\ T_{2_new} &= T_{1_new} + t_2 \\ T_{3_new} &= T_{2_new} + t_3 \\ T_{4_new} &= T_{3_new} + t_4 \\ T_{5_new} &= T_{4_new} + (T_5 - T_4) \\ T_{6_new} &= T_{5_new} + (T_6 - T_5) \\ T_{7_new} &= T_{6_new} + (T_7 - T_6) \end{aligned} \quad (4.12)$$

4.1.2. Case (ii)

In this case, the maximum velocity of the first movement is lower than that of the second movement. Fig. 4.1 illustrates the new velocity profile for this case.

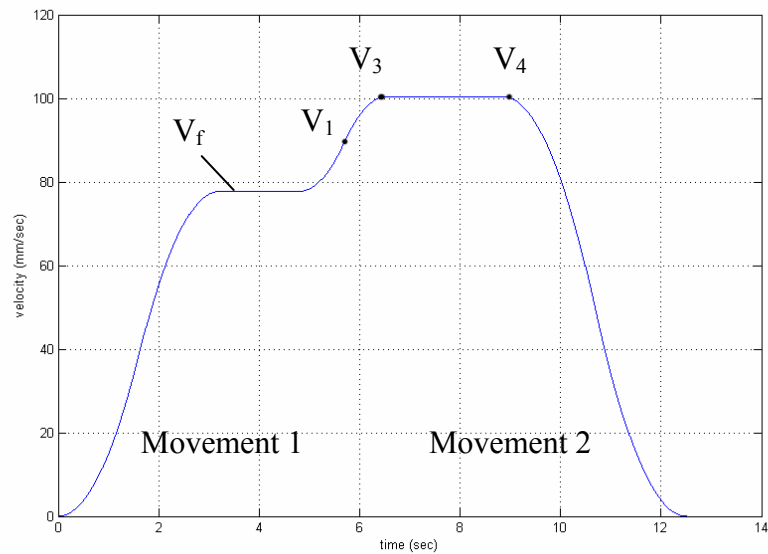


Figure 4.1 New velocity profile of case (ii)

1) Velocity profile of the first movement

The maximum velocity of the first movement is designed to be the final velocity of the movement, which is the same as the starting velocity of the second movement. Since the deceleration stage of the first movement does not exist, segments V, VI, and VII are deleted. Therefore, the time intervals of these three segments are all zero, i.e.,

$$t_5 = 0; t_6 = 0; t_7 = 0 \quad (4.13)$$

The new time interval of segment IV is

$$t_4 = \frac{S_{total-1} - (S_1 + S_2 + S_3)}{V_4} \quad (4.14)$$

2) Velocity profile of the second movement

For the first movement (see Fig. 3.6) to realize the new velocity profile as shown in Fig. 4.1, segment II (see Fig. 3.1) should be eliminated. The time spent from the starting velocity V_f to the final velocity of segment, is determined as

$$t_A = \begin{cases} \sqrt{\frac{2V_f}{J_{\max}}} & V_1 > V_f \\ \frac{(V_f - V_1)}{A_{\max}} & V_2 > V_f \geq V_1 \\ t_3 - \sqrt{\frac{2(V_3 - V_f)}{J_{\max}}} & V_3 > V_f \geq V_2 \end{cases} \quad (4.15)$$

The area below V_f in the acceleration of the original velocity profile is

$$S_{rem} = \begin{cases} \frac{1}{6} J t_A^3 & V_1 > V_f \\ S_1 + \left(V_1 t_A + \frac{1}{2} A_{\max} t_A^2 \right) & V_2 > V_f \geq V_1 \\ S_1 + S_2 + \frac{1}{2} A_1 t_A^2 - \frac{1}{6} J t_A^3 + V_2 t_A & V_3 > V_f \geq V_2 \end{cases} \quad (4.16)$$

Define t_a as half the acceleration time from V_f to V_3 . Since segment II is eliminated and $t_2 = 0$, we can design the time intervals of segments I and III as

$$t_1 = t_3 = t_a \quad (4.17)$$

Then, t_a can be calculated by

$$t_a = \frac{(S_1 + S_2 + S_3 - S_{rem})/2}{(V_f + V_3)/2} \quad (4.18)$$

Define J as the jerk in the deceleration. We then have the following equation

$$\frac{(V_3 - V_f)}{2} = \int_0^{t_a} J dt \quad (4.19)$$

In a similar way to case (i), from Eq (4.19), the jerk can be calculated by

$$J_A = \frac{(V_3 - V_f)}{t_a^2} \quad (4.20)$$

The time interval of segment IV then becomes

$$t_4 = \frac{S_{total-2} - (S_{1_new} + S_{3_new} + S_5 + S_6 + S_7)}{V_4} \quad (4.21)$$

4.1.3. Case (iii)

In this case, the maximum velocities of the two movements are the same. Fig. 4.2 illustrates the new velocity profile of this case. In the first movement, segments V, VI, and VII are deleted, and the new time interval of segment IV is calculated by Eq (4.14). In the second movement, segments I, II, and III are deleted, and the new time interval of segment IV is calculated by Eq. (4.11).

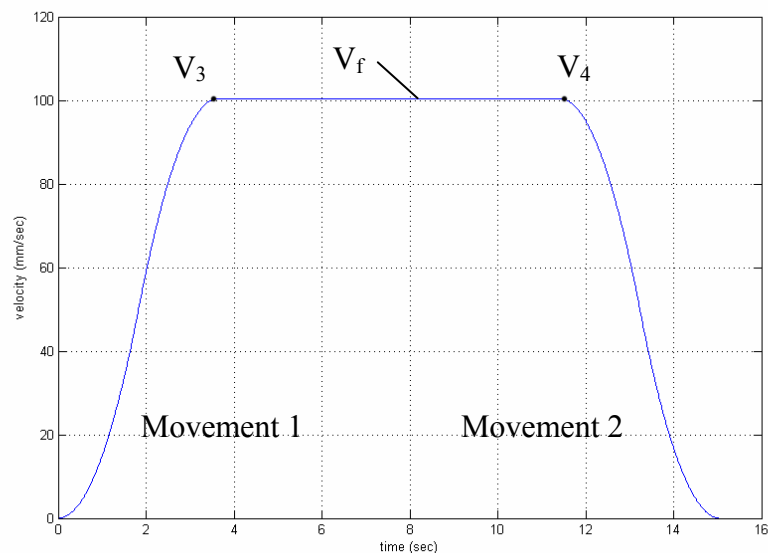


Figure 4.2 New velocity profile of case (iii)

4.2. Motion Planning with Jerk Control

Motion planning with jerk control is developed below and the symbols of the equations are defined in Table 3.1. The new velocity profile generation with jerk control ensures that the jerk is limited within the preset maximum value during the machining process. A proper control of the maximum jerk value helps guarantee the

position and contouring accuracy.

4.2.1. Case (i)

The first movement's (see Fig. 3.6) realisation of the new velocity profile is shown in Fig. 3.7.

1) Velocity profile of the first movement

The velocity profile with a jerk control can be generated in two ways, which depend on the difference between the maximum velocities of the two successive movements. The first way is to shorten segment VI and leave segments V and VII unchanged. The second way is to delete segment VI and shorten segments V and VII.

Define the velocity at half the time of the deceleration stage in the original velocity profile as

$$V_{D_half} = \frac{V_f + V_3}{2} \quad (4.22)$$

If the final velocity of segment V, namely V_5 , is higher than V_{D_half} , the time interval of segment V is not long enough such that its final velocity can decrease down to V_{D_half} , as in Fig. 4.3. In this case, we can modify the velocity profile by shortening the time period of segment VI, since the maximum acceleration has been reached. In contrast, if V_5 is smaller than V_{D_half} , the time interval of segment V is long enough V_5 to decrease down to V_{D_half} , as in Fig. 4.4, and the maximum acceleration cannot be reached. In this case, we can delete segment VI and shorten the time intervals of segments V and VII.

When $V_5 > V_{D_half}$, the time intervals of segments V, VI, and VII are designed as

$$t_5 = T_5 - T_4 \quad (4.23)$$

$$t_6 = \frac{V_5 - V_{6_pro}}{A_{max}} \quad (4.24)$$

$$t_7 = T_7 - T_6 \quad (4.25)$$

where $T_5 \sim T_7$ denote the times at the ends of segments V, VI, and VII in the original velocity profile, as defined in Table 3.1; t_6 is the new time interval of the shortened segment IV, depending on the maximum acceleration A_{max} as well as the proposed resultant velocity at the end of segment VI V_{6_pro} ; V_{6_pro} is determined with the idea that the velocity difference between V_4 and V_5 along the segment V is the same as that between V_{6_pro} and V_f along segment VII. We then derive V_{6_pro} as follows

$$V_{6_pro} = (V_4 - V_5) + V_f \quad (4.26)$$

In Eq (4.24), $V_5 - V_{6_pro}$ denotes the velocity difference along segment VI.

Conversely, when $V_5 \leq V_{D_half}$, segment VI is deleted, and the deceleration stage only contains V and VII. The proposed resultant velocity at the end of segment V, denoted by V_{5_pro} , is designed to be at half the time of the deceleration stage, namely

$$V_{5_pro} = \frac{V_4 + V_f}{2} \quad (4.27)$$

Define the maximum jerk as J_{max} . We then derive V_{5_pro} in the following way

$$V_{5_pro} = V_4 - \int_0^{t_5} J_{max} t dt = V_4 - \frac{1}{2} J_{max} t_5^2 \quad (4.28)$$

It is obvious to see from Eq (4.28) that the jerk control issue is considered when designing the velocity of segment V. Then the time intervals of the segments V, VI, and VII are

$$t_5 = \sqrt{\frac{2(V_{5_pro} - V_3)}{-J_{max}}} \quad (4.29)$$

$$t_6 = t_0; t_7 = t_5 \quad (4.30)$$

Finally, to ensure the moving distance remains unchanged, segment IV is

calculated

$$t_4 = \frac{S_{total-1} - (S_1 + S_2 + S_3 + S_{5_new} + S_{6_new} + S_{7_new})}{V_4} \tag{4.31}$$

The resultant times of seven segments of the first movement can be obtained by Eq (4.9).

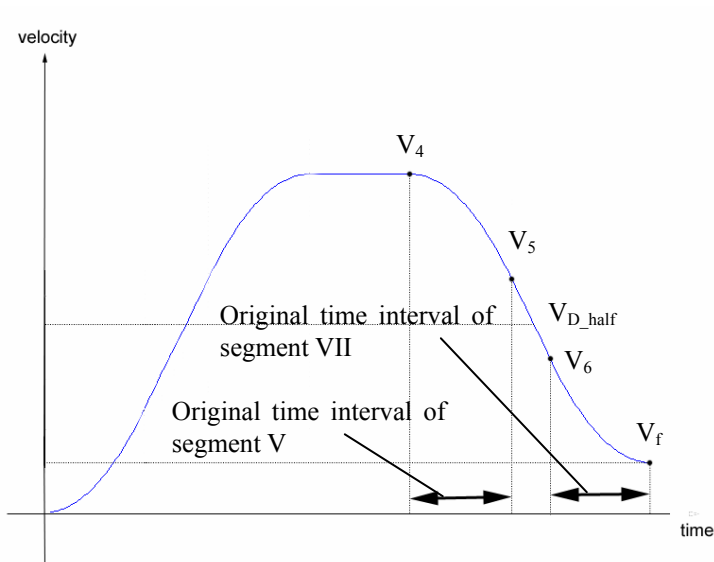


Figure 4.3 The velocity at the end of segment V is higher than the velocity at half the time of the deceleration stage

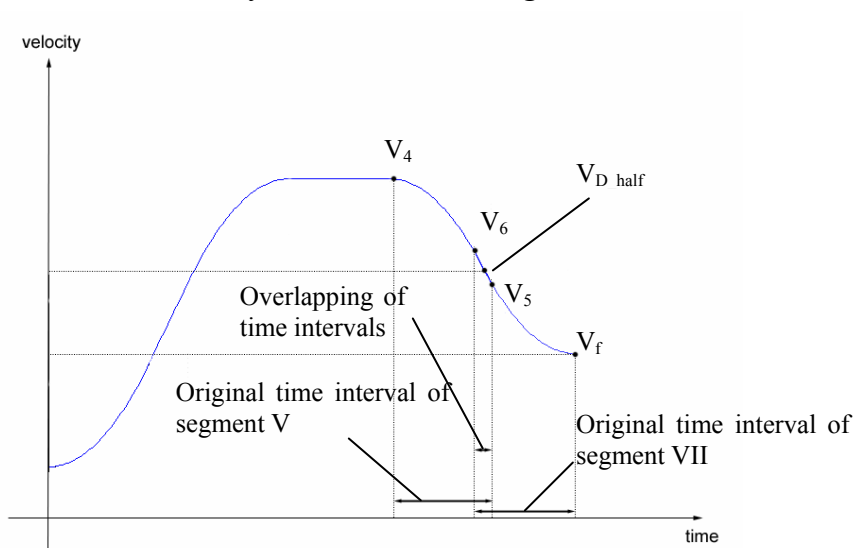


Figure 4.4 The velocity at the end of segment V is lower than the velocity at half the time of the deceleration stage

2) Velocity profile of the second movement

The velocity profile of the second movement is designed in the same way as without the jerk control. Segments I, II, and III are deleted and the time intervals of

segments I, II, and III are zero. The new time interval of segment IV is calculated by Eq (4.11), and the resultant time of seven segments of the second movement is obtained by Eq (4.12).

4.2.2. Case (ii)

In this case, the maximum velocity of the first movement is lower than that of the second movement. Fig. 4.1 illustrates the new velocity profile of this case.

1) Velocity profile of the first movement

The velocity profile of the first movement is designed in the same way as without the jerk control. Segments V, VI, and VII are deleted. The time intervals of these three segments are zero. The new time interval of segment IV is calculated by Eq. (4.14).

2) Velocity profile of the second movement

The velocity profile with a jerk control can be generated in two ways, which depend on the difference between the maximum velocities of the two successive movements. The first way is to shorten segment VI and leave segments V and VII unchanged. The second way is to delete segment VI and shorten segments V and VII. The first half time of the acceleration stage in the original velocity profile is

$$V_{A_half} = \frac{V_f + V_3}{2} \quad (4.32)$$

If the final velocity of segment I, namely V_1 , is smaller than V_{A_half} , the time interval of segment I is not long enough such that its final velocity can increase up to V_{A_half} , as in Fig. 4.5. In this case, we can modify the velocity profile by shortening

the time period of segment II, since the maximum acceleration has been reached. In contrast, if V_I is smaller than V_{A_half} , the time interval of segment I is long enough V_I to increase up to V_{D_half} , as in Fig. 4.6, and the maximum acceleration cannot be reached. In this case, we can delete segment II and shorten the time intervals of segments I and III.

When $V_1 + V_f < V_{A_half}$, the new time intervals of segments I, II, and III are designed as

$$t_1 = T_1 \quad (4.33)$$

$$t_2 = \frac{V_3 - V_f - 2V_1}{A_{\max}} \quad (4.34)$$

$$t_3 = T_2 - T_1 \quad (4.35)$$

where t_2 is determined based on the maximum acceleration A_{\max} .

When $V_1 + V_f \geq V_{A_half}$, segment II is deleted, and the resultant velocity at the end of segment I, denoted by V_{1_pro} , is designed to be at half the time of the acceleration stage, namely

$$V_{1_pro} = \frac{V_3 + V_f}{2} \quad (4.36)$$

which can be further derived in the following way

$$V_{1_pro} = V_f + \int_0^{t_1} J_{\max} t dt = V_f + \frac{1}{2} J_{\max} t_1^2 \quad (4.37)$$

Then, the time intervals of segments I, II, and III are developed as

$$t_1 = \sqrt{\frac{2(V_{1_pro} - V_f)}{J_{\max}}}; \quad t_2 = 0; \quad t_3 = t_1. \quad (4.38)$$

To ensure the moving distance remains unchanged, segment IV is

$$t_4 = \frac{S_{total-2} - (S_{1_new} + S_{2_new} + S_{3_new} + S_5 + S_6 + S_7)}{V_4} \quad (4.39)$$

Note that $S_{2_new} = 0$ for the case when $V_1 \geq V_{A_half}$, where segment II is deleted.

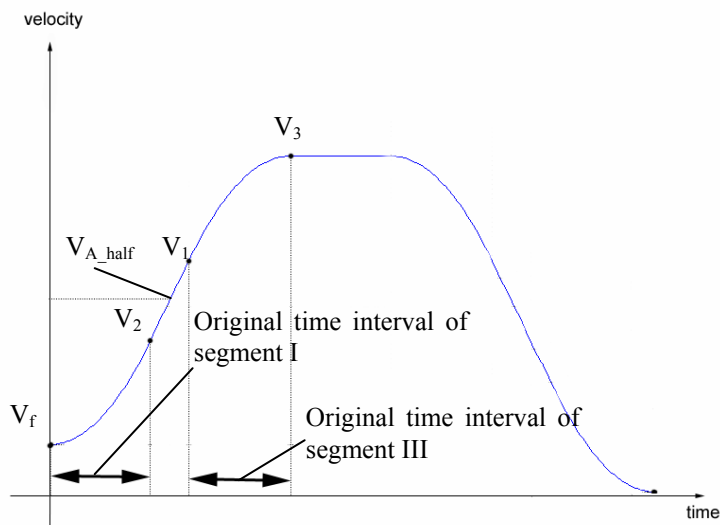


Figure 4.5 The velocity at the end of segment I is lower than the velocity at half the time of the acceleration stage

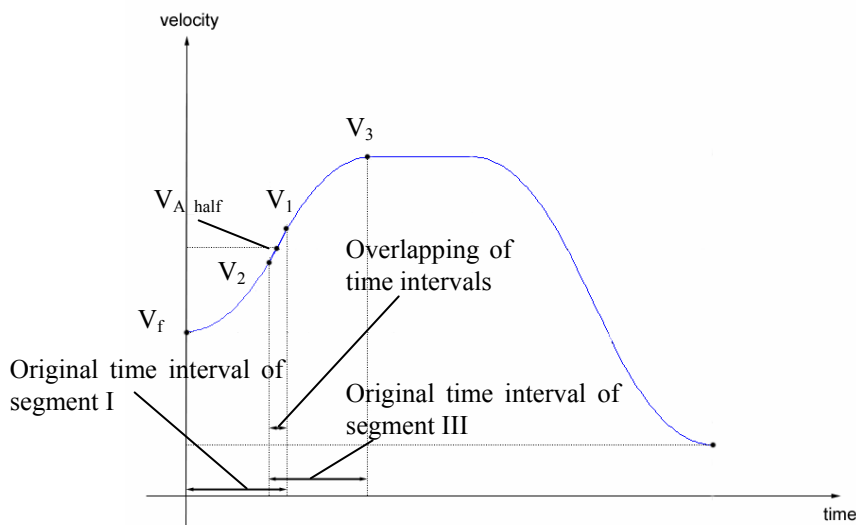


Figure 4.6 The velocity at the end of segment I is higher than the velocity at half the time of the acceleration stage

4.2.3. Case (iii)

Fig. 4.2 illustrates the new velocity profile for the case when the maximum velocities of the two movements are the same. The generation methodology is the same as that without jerk control in section 4.1.3. In the first movement, segments V,

VI, and VII are deleted, and the new time interval of segment IV is calculated by Eq (4.14). In the second movement, segments I, II, and III are deleted, and the new time interval of segment IV is calculated by Eq. (4.11).

4.3. Simulations

Simulations are performed first to demonstrate the effectiveness of the new velocity profiles with jerk control and without jerk controls, respectively. The three cases to be investigated are: (i) maximum velocity of the first movement is higher than the second movement; (ii) maximum velocity of the second movement is higher than the first movement; and (iii) maximum velocity of the first movement is the same as the second movement. The sampling time was 0.01 seconds.

4.3.1. Case (i)

The comparison is based on two different lengths of movements. The first movement is longer than the shorter second movement. The details of motion specification are given in Table 4.1.

Table 4.1 Motion specification simulation in Case (i)

| | |
|----------------------------------|------|
| Distance of first movement (mm) | 300 |
| Distance of second movement (mm) | 10 |
| Jerk (mm/s^3) | 30 |
| Acceleration (mm/s^2) | 30 |
| Velocity (mm/s) | 50 |
| Sampling time (s) | 0.01 |

As the first movement is long enough, maximum velocity is reached in the velocity profile. The second movement is not long enough, and maximum velocity is

not achieved. The maximum velocity of the second movement is treated as the final velocity of the first movement. The total moving distance is 310mm for the two movements.

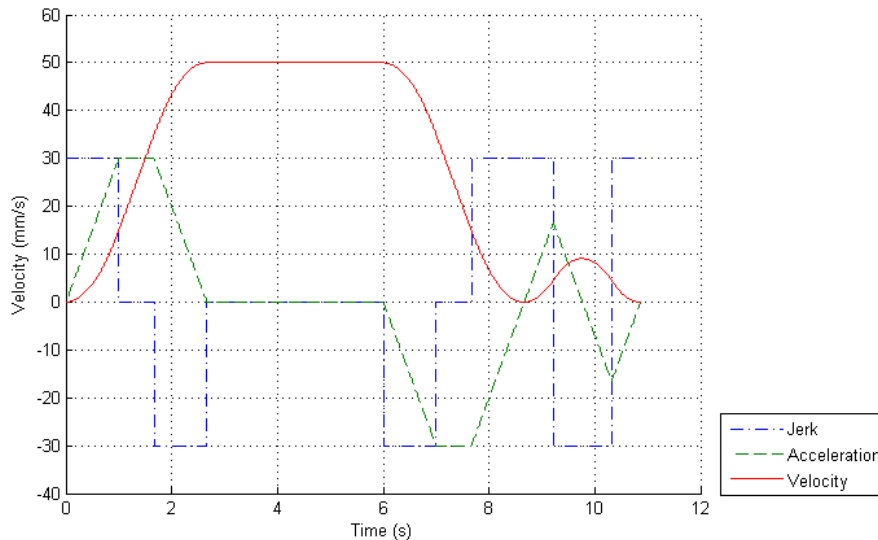


Figure 4.7 Traditional motion planning

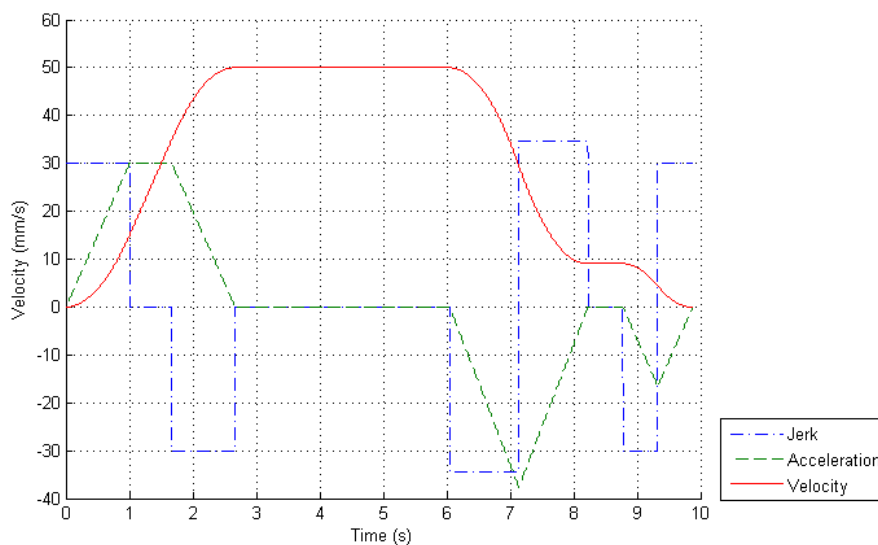


Figure 4.8 New motion planning without jerk control

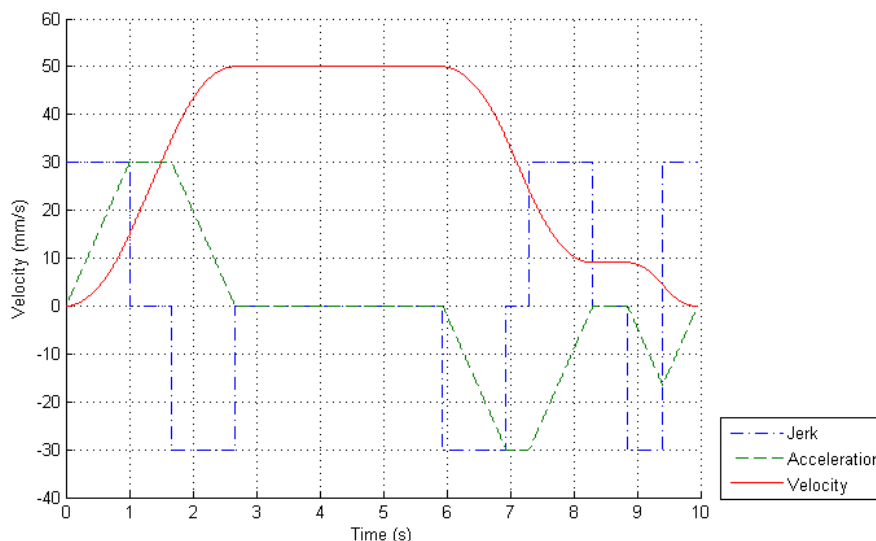


Figure 4.9 New motion planning with jerk control

Figs. 4.7, 4.8, and 4.9 illustrate the velocity profile of the traditional method, the new method without and with jerk control, respectively. It is seen that the spent time without jerk control (9.875 seconds) is a bit shorter than that with jerk control (9.952 seconds), while the traditional method (10.869 seconds) spent the longest time. This is because the jerk of the deceleration stage between the first and the second movement is as high as 34.54mm/s^3 , which exceeds the preset value of 30.0mm/s^3 . When using the method with jerk control, the maximum jerk is well controlled within the limit, as seen in Fig. 4.9.

4.3.2. Case (ii)

The comparison is based on two different lengths of movements. The first movement is shorter than the shorter second movement. The motion specifications are detailed in Table 4.2.

Table 4.2 Motion specification simulation in Case (ii)

| | |
|----------------------------------|------|
| Distance of first movement (mm) | 10 |
| Distance of second movement (mm) | 300 |
| Jerk (mm/s^3) | 30 |
| Acceleration (mm/s^2) | 30 |
| Velocity (mm/s) | 50 |
| Sampling time (s) | 0.01 |

The first movement is not long enough and thus the maximum velocity cannot be reached. The second movement is long enough and the maximum velocity can be reached. As seen in Figs. 4.10, 4.11, and 4.12, the maximum velocity of the first movement is treated as the final velocity of the first movement. The total distance is 310mm for the two movements.

Figs. 4.10, 4.11, and 4.12 illustrate the velocity profiles of the traditional method, the new method without and with jerk control, respectively. Fig. 4.11 illustrates the velocity profile without jerk control, taking a slightly shorter time of 9.875 seconds. In this case, there is no jerk control. The maximum jerk during the acceleration stage at the connection between the first and second movements reaches 34.54mm/s^3 , which exceeds the preset value of 30.0mm/s^3 . Fig 4.12 illustrates the velocity profile with jerk control, taking a time of 9.952 seconds. Due to the introduction of jerk control, the maximum jerk does not exceed the preset value. Furthermore, Fig 4.10 illustrates the velocity profile of the traditional method, and it spent the longest time among the three methods (10.869 seconds).

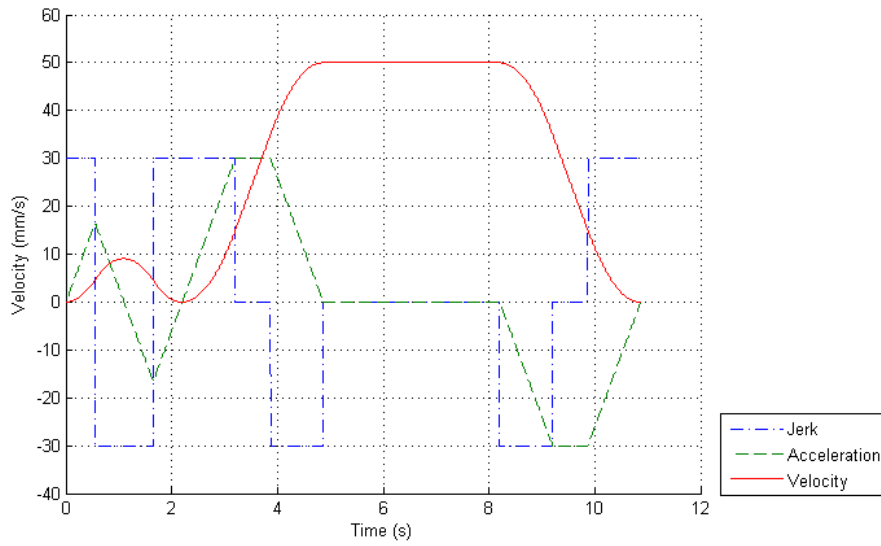


Figure 4.10 Traditional motion planning

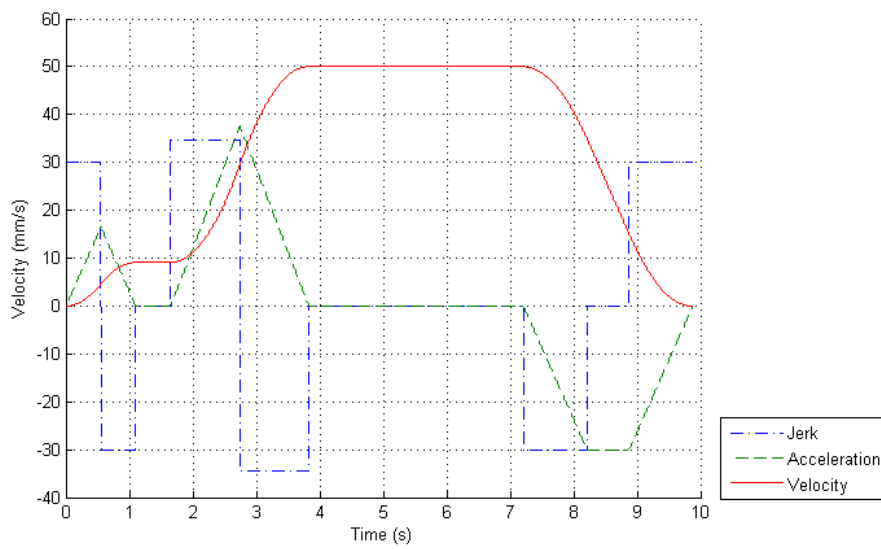


Figure 4.11 New motion planning without jerk control

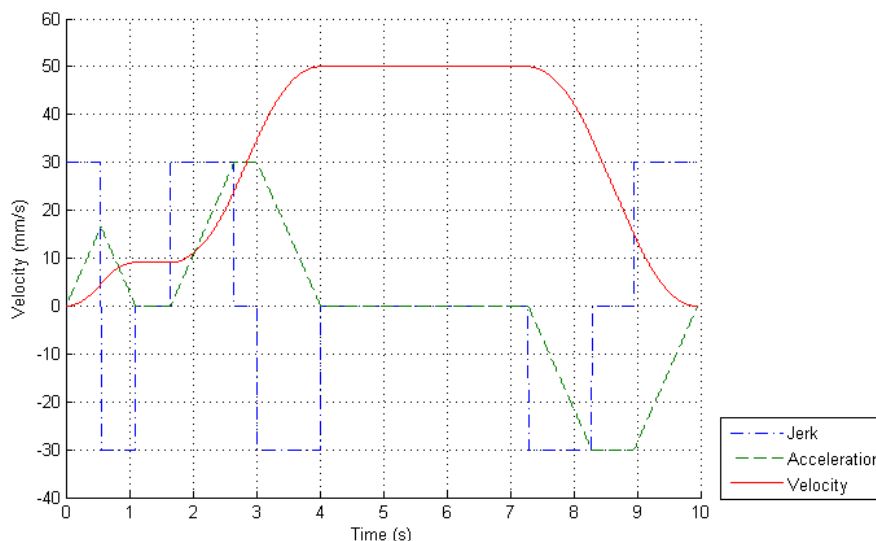


Figure 4.12 New motion planning with jerk control

4.3.3. Case (iii)

In this case, the distances of two movements are the same, i.e. 300mm each. As both the movements are long enough for achieving maximum velocity, the final velocity can be set as the maximum velocity of either the first movement or second movement. The motion specification of the movements is described in Table 4.3.

Table 4.3 Motion specification simulation in Case (iii)

| | |
|----------------------------------|------|
| Distance of first movement (mm) | 300 |
| Distance of second movement (mm) | 300 |
| Jerk (mm/s^3) | 30 |
| Acceleration (mm/s^2) | 30 |
| Velocity (mm/s) | 50 |
| Sampling time (s) | 0.01 |

Figs. 4.13, 4.14, and 4.15 illustrate the velocity profiles of the traditional method, the new method without and with jerk control, respectively. This is a special case because it is identified that results of the two methods without and with jerk control are the same. There is no acceleration/deceleration stage between the two

movements. The time spent by the two methods is 14.668 seconds, while the traditional method spent 17.334 seconds.

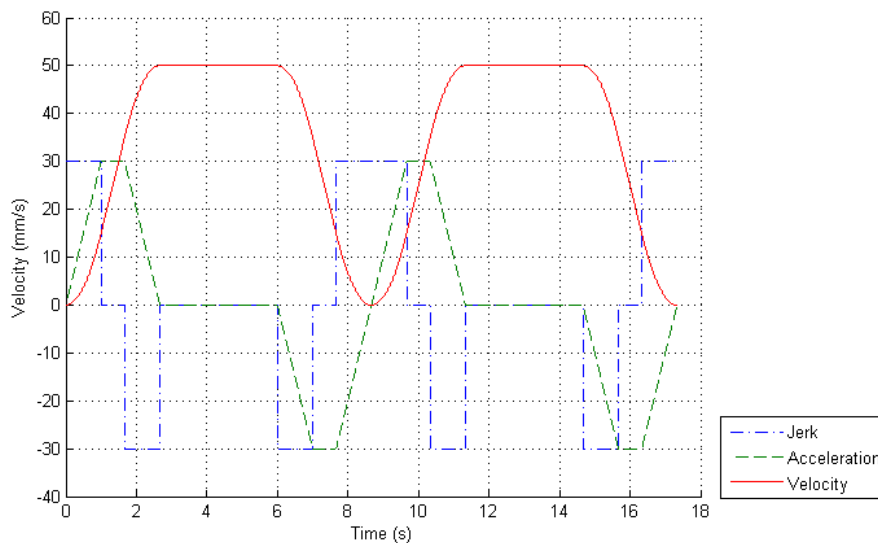


Figure 4.13 Traditional motion planning

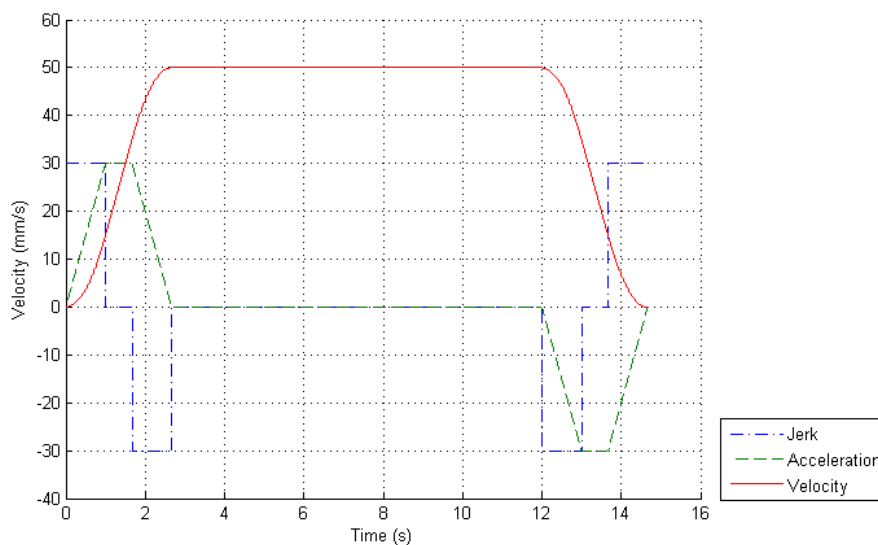


Figure 4.14 New motion planning without jerk control

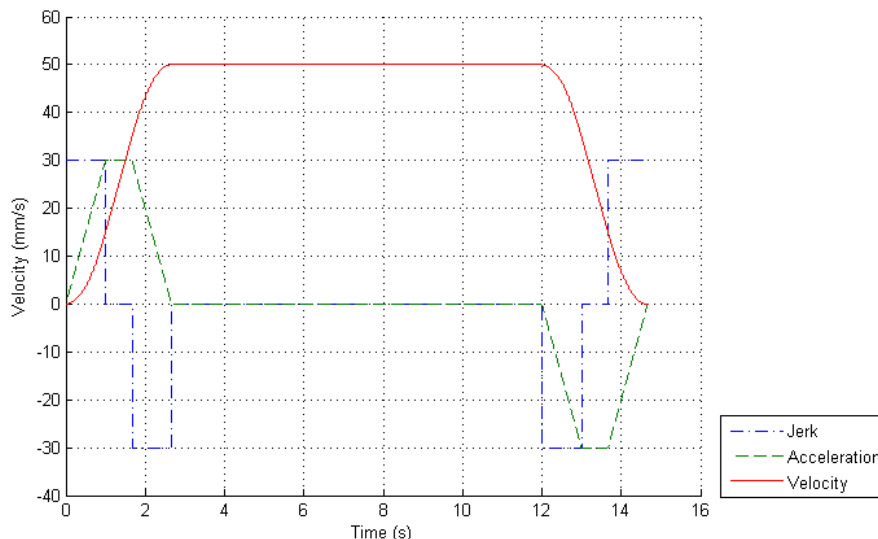


Figure 4.15 New motion planning with jerk control

4.3.4. Relationship of Time Saving and the Continuity of the Trajectory

The time saving of the proposed new velocity profile depends on the continuity of the trajectory. Fig. 4.16 shows the trajectory of a rectangle. As the lines are connected with sharp angles, the new velocity profiles cannot be applied, and the time spent in movement is the same as the traditional method, which is 4 seconds. Fig. 4.17 shows a trajectory of four steps connecting in tangent without sharp angles, where the new velocity profile can be applied, and the time is saved. The operation time by the proposed velocity profile is 2.5 seconds, while that by the traditional method is 4 seconds. The simulation specifications are tabled in Table 4.4.

Table 4.4 Motion specification

| | |
|--|------|
| Distance of step 1, 2, 3, and 4 (mm) | 10 |
| Jerk (mm/s^3) | 500 |
| Acceleration (mm/s^2) | 50 |
| Velocity of step 1, 2, 3, and 4 (mm/s) | 37.5 |

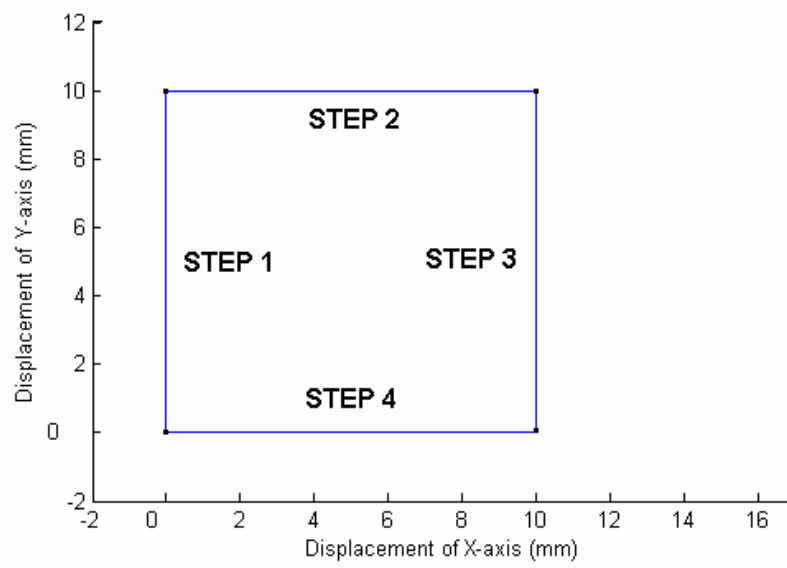


Figure 4.16 Trajectory with sharp corners

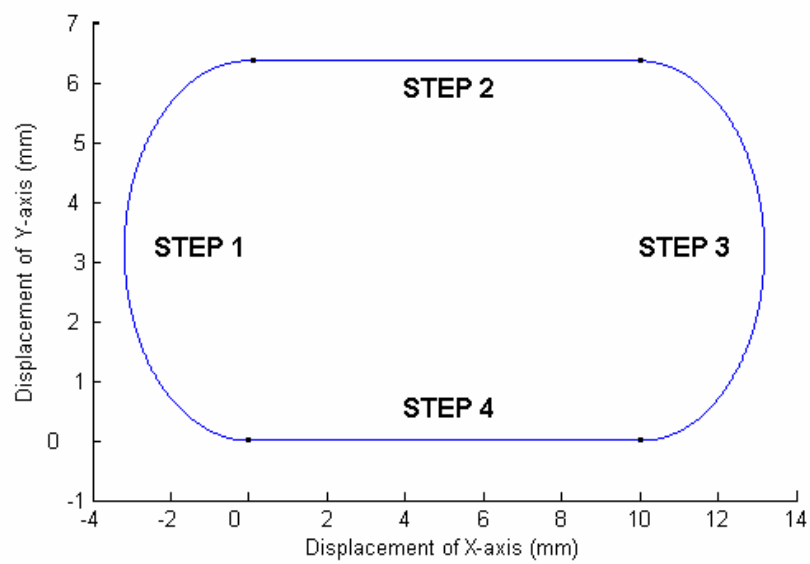


Figure 4.17 Trajectory without sharp corners

Chapter 5. Experiments

In this chapter, experiments are performed to demonstrate the effectiveness of the proposed velocity profile generation approaches.

5.1. Experiments Setup

Figs. 5.1-5.3 illustrate the homemade 5-axis CNC machine, which is supported by the Innovation and Technology Fund of Hong Kong. The machine employs a TTTRR structure, with three translational axes (X-, Y- and Z-axis) and two rotational axes (A-, C-axis). The X, Y, and Z translational axes are driven by DC brushless motors with a DCT0040 [<http://www.dynacitytech.com>] motion controller/driver, and the two rotational axes A and C are driven by brushed motors with a DCT0020 [<http://www.dynacitytech.com>] motor controller/driver [57]. The sampling frequencies of the position and current control loops are 4 and 20 kHz, respectively. The specification of the machine is listed in table 5.1.



Figure 5.1 Outlook of the homemade 5-axis CNC machine

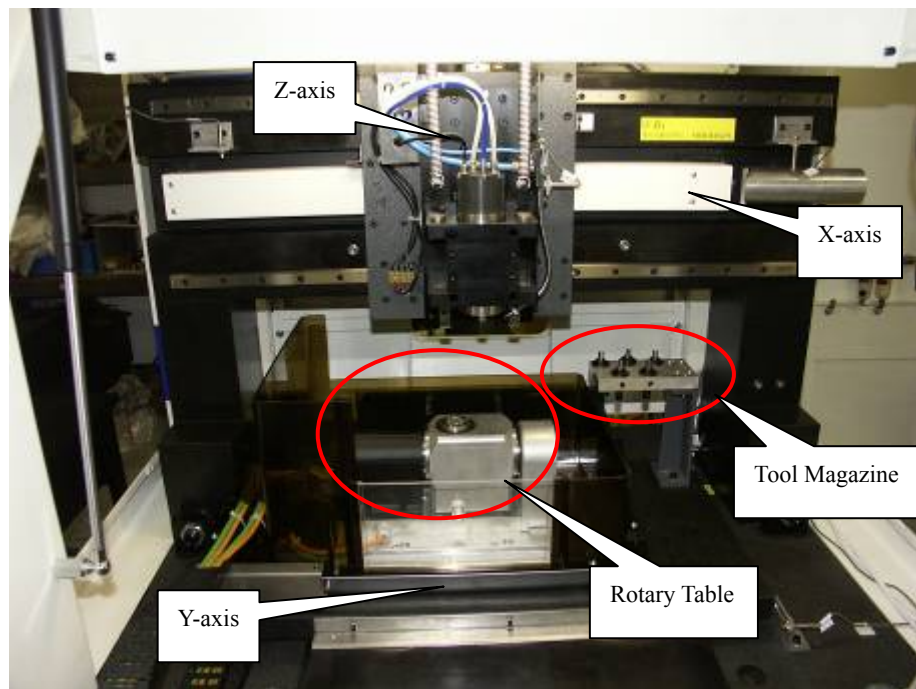


Figure 5.2 Frame of the CNC machine

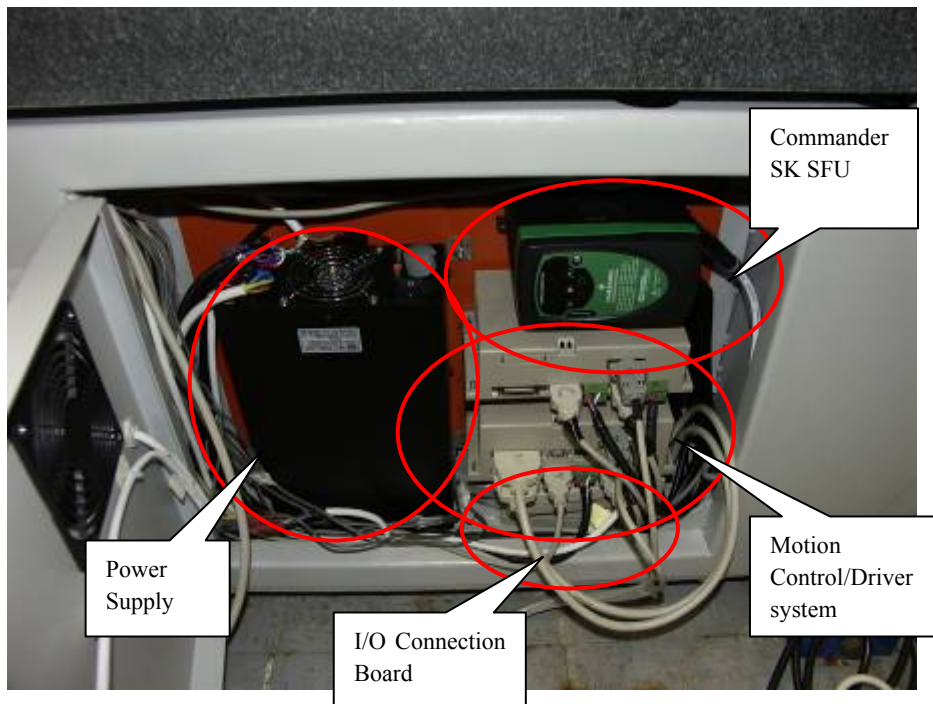


Figure 5.3 Motion and control system of the CNC machine

Table 5.1 Specifications of the developed 5-axis machine

| 5-axis Machine | |
|------------------------------|---|
| Machine Dimensions | 1260mm (L) x 1340mm (W) x 1680mm (H) |
| Machine Frame Dimensions | 1060mm (L) x 1000mm (W) x 1167mm (H) |
| X-axis Traveling Distance | 600mm (with tool magazine) 300mm (without tool magazine) |
| Y-axis Traveling Distance | 450mm |
| Z-axis Traveling Distance | 162mm |
| A-axis Travelling Distance | 0° ~ ±90° |
| C-axis Travelling Distance | 0° ~ ±360° |
| Working Table | 700mm x 400mm Diameter 65mm (rotary table) |
| Spindle | High Speed Spindle Model: PRT210 |
| Spindle Revolution | 18,000 ~ 55,000 RPM (700W) |
| Frequency Converter | Commander SK |
| CNC System Precision | 0.5µm (X-, Y-axis) and 1µm (Z-axis) 0.0018° (A-axis) and 0.0018° (C-axis) |
| Repeat Orientation Precision | 1µm (X-, Y-axis) and 2µm (Z-axis) |
| Orientation Precision | 1µm (X-axis, Y-axis) and 2µm (Z-axis) |
| Spindle Cooling System | Coolant fluid |
| Cutting Cooling System | Oil |
| CNC Control System | DCT0040 Motion Control / Driver System DCT0020 Motion Control / Driver System CNC Application Package |
| Motors | 3 DC brushless motors 2 DC brushed motors |
| Tool Magazine | For storing five cutting tools |
| Power Supply Voltage | AC 220V 50Hz |

The control application code is written in C and ASM language, running in the digital signal processor (DSP). A window utility program developed by Visual C++ enables us to quickly set up, configure, and troubleshoot controllers. The experimental data (i.e. position and velocity) can be obtained in real time from the control system.

5.2. Experimental Results

In the experiment, we engraved a shape on the surface of a hardwood, as seen in Fig. 5.4. The motion trajectory in the X-Y plane is shown in Fig. 5.5, with the maximum acceleration and jerk of 50 mm/s^2 and 500 mm/s^3 , respectively. The contour error was calculated by the shortest distance between the actual position measured by the motor encoder and the desired trajectory path. The traditional velocity profile and the new velocity profile with and without jerk control were implemented for comparison. Three trials for each method have been taken in the experiment. The NC code for engraving along the trajectory is given as follows.

```
G1X6.042Y22.548F600.  
G2X6.292Y22.922I0.676J-0.181  
G1X8.811Y24.855  
G2X9.238Y25.10.426J-0.555  
G1X11.768  
G2X16.098Y22.5I0.J-5.  
G1X18.985Y17.5  
G3X23.315Y15.14.33J2.5  
G1X23.8  
G3X28.8Y20.I0.J5.  
G1Y20.5  
X29.3  
G2X34.3Y15.5I0.J-5.  
G1Y14.349  
G2X31.888Y5.349I-18.J0.  
G1X31.398Y4.5  
G2X23.604Y0.I-7.794J4.5  
G1X0.
```



Figure 5.4 Machined part

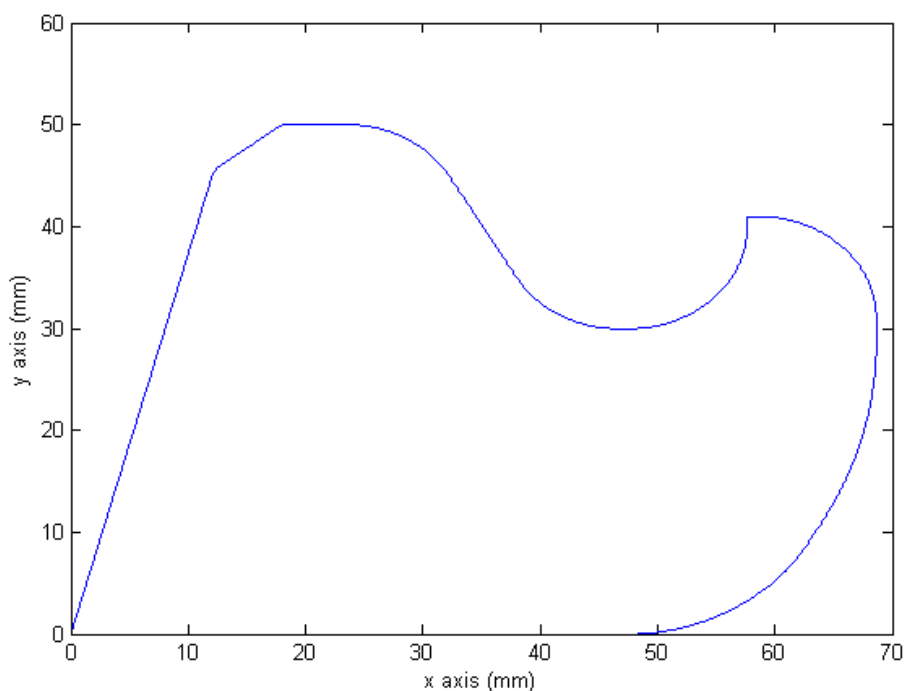


Figure 5.5 Trajectory path in X-Y plane

5.2.1. Application of Traditional Velocity Profile

The traditional motion planning method was firstly performed for the trajectory. Fig. 5.6 illustrates the x-axis, y-axis, and resultant velocity profiles of second trial. It is seen that the traditional velocity profile requires an operation time of 16.05 seconds, and the machine tool stopped 17 times at the connection of movements. Fig.

5.7 illustrates the x-axis and y-axis position errors, and the contour error of second trial. The average maximum x-axis and y-axis position errors are 0.031mm and 0.029mm, respectively. The average maximum contour error is 0.011mm for the traditional method. Table 5.2 gives a comparison of the errors of three trials.

Table 5.2 Comparison of results of traditional motion planning

| | 1 st Trial | 2 nd Trial | 3 rd Trial | Average |
|------------------------------------|-----------------------|-----------------------|-----------------------|---------|
| Maximum x-axis position error (mm) | 0.030 | 0.032 | 0.030 | 0.031 |
| Maximum y-axis position error (mm) | 0.029 | 0.031 | 0.028 | 0.029 |
| Maximum contour error (mm) | 0.008 | 0.013 | 0.012 | 0.011 |

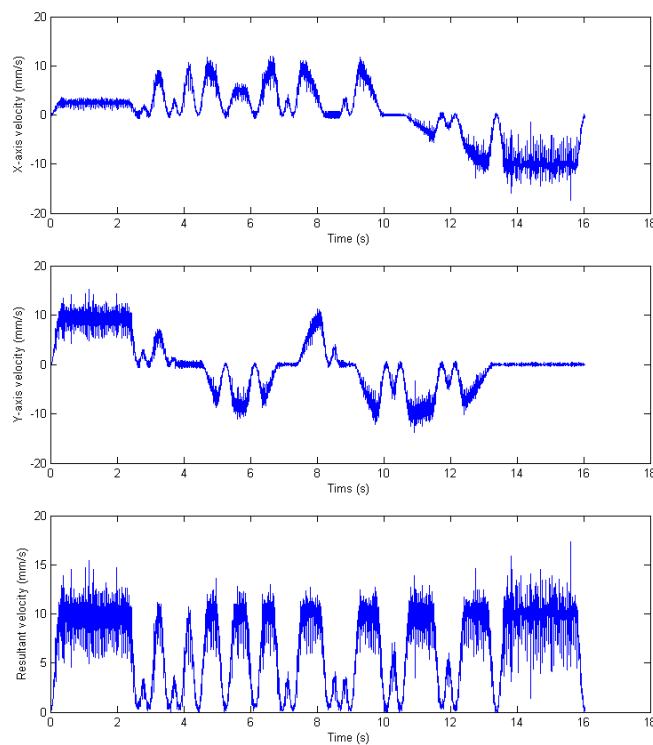


Figure 5.6 Velocity profiles of traditional motion planning

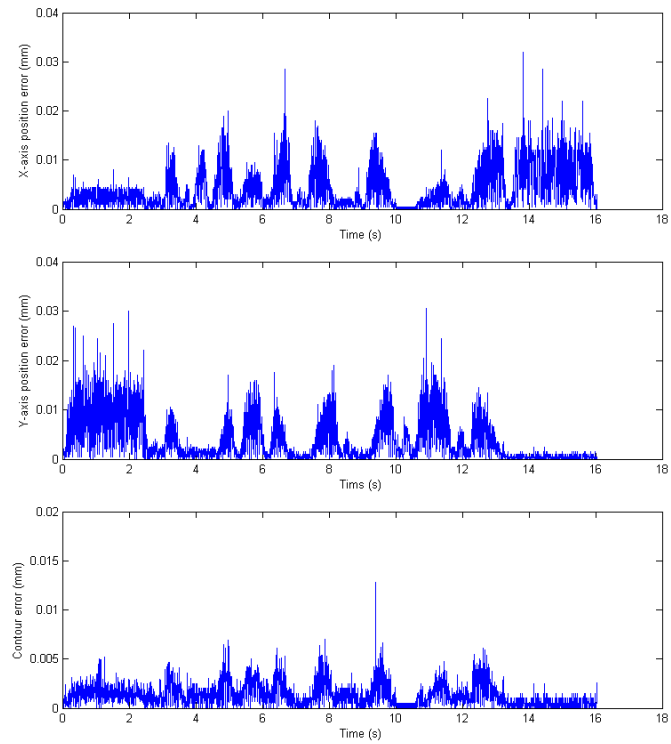


Figure 5.7 Position errors and contour error of traditional motion planning

5.2.2. Application of New Velocity Profile without Jerk Control

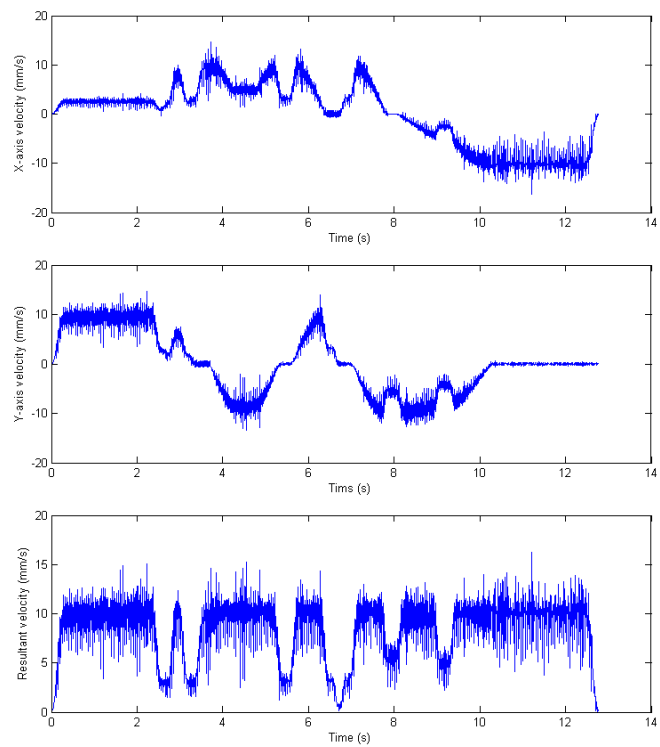


Figure 5.8 Velocity profiles of new motion planning without jerk control

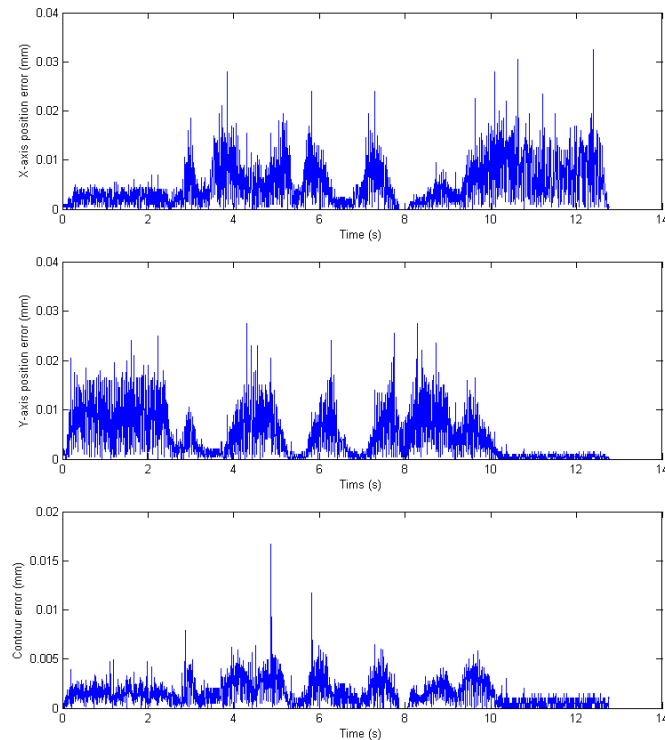


Figure 5.9 Position errors and contour error of new motion planning without jerk control

Fig. 5.8 illustrates the x-axis, y-axis, and resultant velocity profiles of second trial. It is seen that the new velocity profile without jerk control requires an operation time of 12.77 seconds, which spent less operation time than the traditional method. The machine tool stopped only 1 time at the connection of movements. Fig. 5.9 illustrates the x-axis and y-axis position errors and the contour error of second trial. The average maximum x-axis and y-axis position errors are 0.032mm and 0.028mm, respectively. The average maximum contour error is 0.014mm for the new method without jerk control. The position and contour errors are slightly higher than the traditional method, caused by the exceeded limit jerk being employed. Table 5.3 gives a comparison of the errors of three trials.

Table 5.3 Comparison of results of new motion planning without jerk control

| | 1 st Trial | 2 nd Trial | 3 rd Trial | Average |
|------------------------------------|-----------------------|-----------------------|-----------------------|---------|
| Maximum x-axis position error (mm) | 0.031 | 0.033 | 0.032 | 0.032 |
| Maximum y-axis position error (mm) | 0.028 | 0.028 | 0.029 | 0.028 |
| Maximum contour error (mm) | 0.012 | 0.017 | 0.013 | 0.014 |

5.2.3. Application of New Velocity Profile with Jerk Control

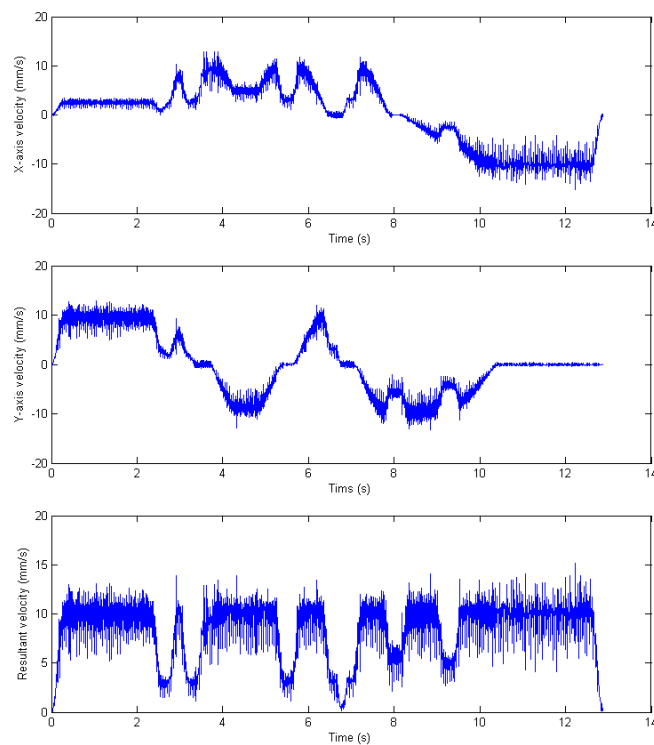


Figure 5.10 Velocity profiles of new motion planning with jerk control

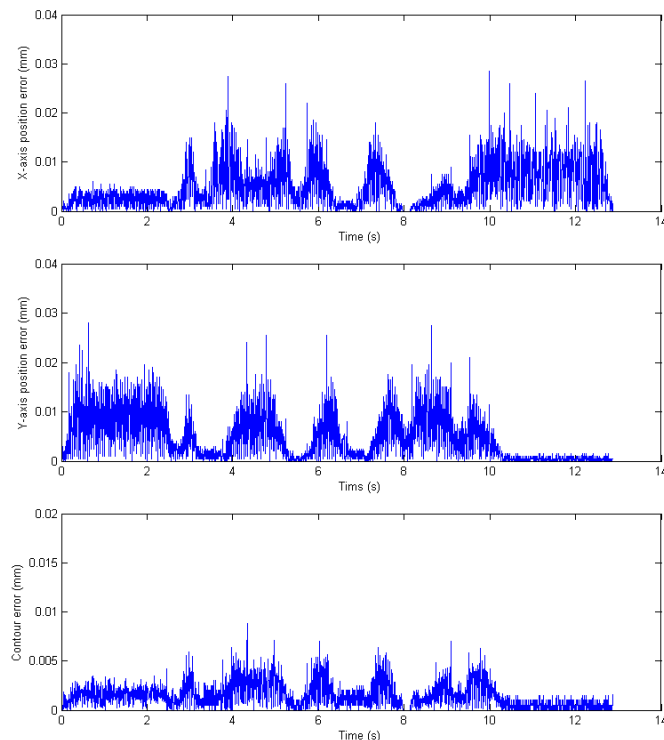


Figure 5.11 Position errors and contour error of new motion planning with jerk control

Fig. 5.10 illustrates the x-axis, y-axis, and resultant velocity profiles of second trial. It is seen that the new velocity profile with jerk control requires an operation time of 12.88 seconds, which spent less operation time than the traditional method but a bit longer than the new method without jerk control. The machine tool stopped 1 time at the connection of movements. Fig. 5.11 illustrates the x-axis and y-axis position errors, and the contour error of second trial. The average maximum x-axis and y-axis position errors are 0.031mm and 0.028mm, respectively. The average maximum contour error is 0.011mm for the new method with jerk control. Table 5.4 gives a comparison of the errors of three trials.

Table 5.4 Comparison of results of new motion planning with jerk control

| | 1 st Trial | 2 nd Trial | 3 rd Trial | Average |
|------------------------------------|-----------------------|-----------------------|-----------------------|---------|
| Maximum x-axis position error (mm) | 0.032 | 0.029 | 0.031 | 0.031 |
| Maximum y-axis position error (mm) | 0.029 | 0.028 | 0.028 | 0.028 |
| Maximum contour error (mm) | 0.015 | 0.009 | 0.010 | 0.011 |

5.3. Discussions

The experiment results show that the new velocity profiles require less operation time and thus improve working efficiency compared to the traditional velocity profile. The new velocity profile without jerk control requires less operation time than the method with jerk control, but results in a slightly higher position and contour errors than the traditional method, due to employing high jerk at the connection of movements. By introducing jerk control, the new velocity profile requires a little more operation time than that without jerk control, but leads to better motion performance that is compatible to that of the traditional velocity profile. Table 5.5 gives a comparison of the results with the three velocity profiles.

Table 5.5 Comparison of results

| | Traditional velocity profile | New velocity profile without jerk control | New velocity profile with jerk control |
|------------------------------------|------------------------------|---|--|
| Operation time (second) | 16.05 | 12.77 | 12.88 |
| Time saved (%) | | 20.4% | 19.8% |
| 1 st Trial | | | |
| Maximum x-axis position error (mm) | 0.030 | 0.031 | 0.032 |
| Maximum y-axis position error (mm) | 0.029 | 0.028 | 0.029 |
| Maximum contour error (mm) | 0.008 | 0.012 | 0.015 |
| 2 nd Trial | | | |
| Maximum x-axis position error (mm) | 0.032 | 0.033 | 0.029 |
| Maximum y-axis position error (mm) | 0.031 | 0.028 | 0.028 |
| Maximum contour error (mm) | 0.013 | 0.017 | 0.009 |
| 3 rd Trial | | | |
| Maximum x-axis position error (mm) | 0.030 | 0.032 | 0.031 |
| Maximum y-axis position error (mm) | 0.028 | 0.029 | 0.028 |
| Maximum contour error (mm) | 0.012 | 0.013 | 0.010 |
| Average of three trials | | | |
| Maximum x-axis position error (mm) | 0.031 | 0.032 | 0.031 |
| Maximum y-axis position error (mm) | 0.029 | 0.028 | 0.028 |
| Maximum contour error (mm) | 0.011 | 0.014 | 0.011 |

Chapter 6. Conclusions

In this thesis, a new velocity profile generation methodology is developed for improving CNC machining efficiency without degrading motion accuracy. The velocity does not decelerate to zero at the connection of successive movements in the proposed motion planning. The advantages of the new velocity profile are twofold. First, it can be implemented easily and effectively, without demanding for large buffer and complex facility to process huge amount of look-ahead commands. Second, it shortens the operation time via “smoothing” successive movements but not increasing the maximum velocity of each movement, and therefore does not degrade the motion accuracy. Moreover, the proposed new velocity profile can better deal with the successive machining of little line segments, in which the given maximal velocity is limited by the given short distance of each movement.

The new velocity profiles with and without jerk control are developed, respectively. With the method without jerk control, the jerk may exceed the preset maximum value during the machining process. The method with jerk control can control the jerk within limited maximum jerk. The S-curve velocity profile and the Acceleration/Deceleration Before Interpolation are adopted in the study, while the S-curve velocity profile is generated based on the polynomial selection. Simulations are performed to demonstrate that both the new velocity profiles without and with jerk control require less machining time than the traditional velocity profile, and the new velocity profile with jerk control can also control the jerk to be within the

required range.

Experiments are further performed on a home-made multi-axis CNC machine tool to demonstrate the effectiveness of the proposed approach. The machining task in the experiment is to machine a list of circular arc and straight line segments, either connected continuously or in sharp angle. Experimental results show that the new velocity profiles require less operation time than the traditional velocity profile. The new velocity profile without jerk control requires less operation time, but results in slightly higher position and contour errors. The new velocity profile associated with jerk control exhibits satisfactory comprehensive performance in terms of motion efficiency and accuracy.

References

- [1] Hindustan Machine Tools Limited, "Mechatronics and Machine Tools", McGraw Hill, 1999
- [2] D. J. Petrone, and M. D. Stackhouse, "PC-based Control Goes Real-time", *Control Engineering*, vol. 45, no. 6, pp.54-64, April 1998
- [3] X. B. Ma, Z. Y. Han, Y. Z. Wang, and H. Y. Fu, "Development of a PC-based Open Architecture Software-CNC software", *Chinese Journal of Aeronautics*, vol. 20, pp. 272-281, 2007
- [4] Y. Koren, and R. S. Lin, "Five-axis Surface Interpolators", *CIRP Annals – Manufacturing Technology*, vol. 44, pp.379-382, 1995
- [5] X. Yi, H. Qi, Q. Liu, and X. Yi, "Tool Path Generation of 5-axis CNC Whirlwind Milling Model for Freeform Surfaces", *Proceedings of the 2005 IEEE International Conference on Mechatronics & Automation*, Niagara Falls, Canada, pp.537-540, July 2005
- [6] X. Yi, Y. Lin, S. Fu, J. Zhou, and X. Hu, "5-axis CNC Whirlwind Milling Model for Complex Freeform Surfaces", *Proceedings of the 2006 IEEE International Conference on Mechatronics and Automation*, Luoyang, China, pp.1953-1957, June 2006
- [7] S. Makhanov, "Optimization and Correction of the Tool Path of the Five-axis Milling Machine Part 1. Spatial Optimization", *Mathematics and Computers in Simulation*, vol. 75, pp.210-230, 2007
- [8] C. C. Lo, "A New Approach to CNC Tool Path Generation", *Computer-Aided Design*, vol. 30, no. 8, pp.649-655, 1998
- [9] F. Gravot, Y. Hirano, and S. Yoshizawa, "Generation of "Optimal" Speed Profile for Motion Planning", *Proceedings of the 2007 IEEE/RSJ International Conference on Intelligent Robots and Systems*, San Diego, CA, USA, pp.4071-4076, Oct 2007
- [10] Z. Y. Zhao, C. Y. Wang, H. M. Zhou, and Z. Qin, "Pocketing Toolpath Optimization for Sharp Corners", *Journal of Materials Processing Technology*, vol. 192-193, pp.175-180, October 2007

-
-
- [11] J. E. Bobrow, "Optimal Robot Path Planning Using the Minimum-Time Criterion", *IEEE Journal of Robotics and Automation*, vol. 4, no. 4, pp.443-450, 1988
- [12] J. W. Hong, Y. O. Kim, and I. J. Ha, "Simplified Time-Optimal Path Planning of X-Y Gantry Systems Along Circular Paths", *Automatica*, vol. 44, pp.149-156, 2008
- [13] S. D. Timar, R. T. Farouki, T. S. Smith, and C. L. Boyadjieff, "Algorithms for Time-Optimal Control of CNC Machines Along Curved Tool Paths", *Robotics and Computer-Integrated Manufacturing*, vol. 21, pp.37-53, 2005
- [14] S. D. Timar, and R. T. Farouki, "Time-optimal Traversal of Curved Paths by Cartesian CNC Machines Under Both Constant and Speed-Dependent Axis Acceleration Bounds", *Robotics and Computer-Integrated Manufacturing*, vol.23, pp.563-579, 2007
- [15] Y. Liu, J. Xu, Z. Li, "Development and Implementation of NURBS Interpolator with Look-ahead Technique", *Proceedings of the 3rd Annual IEEE Conference on Automation Science and Engineering*, Scottsdale, AZ, USA, pp.134-139, September 2007
- [16] H. T. Yau, J. B. Wang, and W. C. Chen, "Development and Implementation for Real-Time Look-ahead Interpolator by Using Bezier Curve to Fit CNC Continuous Short Blocks", *Proceedings of 2006 IEEE International Conference on Mechatronics*, Taipei, Taiwan, pp.78-83, 2005
- [17] C. H. Huang, "The Feedrate Control of CNC Machine Tools", Master Thesis, National Central University, 2002
- [18] "Series 16i/ 18i/ 160i/ 180i/ 160is/ 180is – MA for Machining Center Operator's Manual", FANUC, 2000
- [19] "SINUMERIK 840D sl/840Di sl/840D/840Di/810D Basic Logic Functions: Continuous-path Mode, Exact Stop, Look-ahead Function Manuel", SIEMENS, 2006
- [20] K. Erkorkmaz, C. H. Yeung, and Y. Altintas, "Virtual CNC system. Part II. High Speed Contouring Application", *International Journal of Machine Tools & Manufacturing*, vol. 46, pp.1124-1138, 2006
- [21] C. M. Lam, "Development of a Hybrid Control System using NURBS Interpolator and Cross-Coupling Approach to Eliminate Contour Error: Theory and Application", MPhil Thesis, City University of Hong Kong, 2006
- [22] T. Schuett, "A Closer Look At Look-Ahead", <http://www.mmsonline.com/articles/039603.html>, 2003

-
-
- [23] S. Brock, and T. Kaczmarek, "2-D Command Preprocessor with Jerk Limit for Machine Tools Driver", Proceedings of IEEE International Symposium on Industrial Electronics, Warsaw, Poland, pp.230-235, Jun 1996
- [24] J. S. Gyorfi, and C. H. Wu, "A Minimum-Jerk Speed Planning Algorithm for Coordinated and Control of Automated Assembly Manufacturing", vol. 3, no. 4, pp. 454-462, October 2006
- [25] K. C. Koh, H. S. Aum, and H. S. Cho, "A Minimum-time Motion Planning Method based on Phase Space Analysis", Proceedings of the 1999 IEEE International Conference on Control Application, Kohala Coast-Island of Hawaii, Hawaii, USA, pp.273-278, 1999
- [26] S. H. Nam, and M. Y. Yang, "A Study on a Generalized Parametric Interpolator with Real-time Jerk-limited Acceleration", Computer-Aided Design, vol. 36, pp.27-36, 2004
- [27] X. Liu, F. Ahmad, K. Yamazaki, and M. Mori, "Adaptive Interpolation Scheme for NURBS Curves with the Integration of Machining Dynamics", International Journal of Machine Tools & Manufacture, vol. 45, pp.433-444, 2005
- [28] Y. F. Chang, "Design and Implementation of a Linear Jerk Filter for a Computerized Numerical Controller", Control Engineering Practice, vol. 13, pp.567-576, 2005
- [29] J. Dong, P. M. Ferreira, and J. A. Stori, "Feed-rate Optimization with Jerk Constraints for Generating Minimum-Time Trajectories", International Journal of Machine Tools & Manufacture, vol.47, pp.1941-1955, 2007
- [30] K. Erkorkmaz, and Y. Altintas, "High Speed CNC System Design. Part I: Jerk Limited Trajectory Generation and Quintic Spline Interpolation", International Journal Tools & Manufacture, vol. 41, pp.1323-1345, 2001
- [31] R. L. Racicot, "Limiting Servo Motor Torque Gradients with Near Minimum Time Response", IEEE Transactions on Control Systems Technology, vol. 1, no. 4, pp.284-289, 1993
- [32] K. J. Kyriakopoulos, and G. N. Saridis, "Minimum Jerk path Generation", Proceedings of the 1988 IEEE International Conference on Robotics and Automation, Philadelphia, PA, USA, pp.364-369, 1988
- [33] S. A. Bazaz, and B. Tondu, "Minimum Time On-line Joint Trajectory Generator Based on Low Order Spline Method for Industrial Manipulators", Robotics and Autonomous Systems, vol.29, pp.257-268, 1999
- [34] W. J. Chang, "Acceleration/ Deceleration Planning with Jerk Limitation for Multi-Axis Motion Control", Master Thesis, National Central University, 2002

-
-
- [35] M. Shpitalni, Y. Koren, and C. C. Lo, "Real time Curve Interpolators", *Computer-Aided Design*, vol. 26, no. 11, pp.832-838, November 1994
- [36] M. Y. Cheng, M. C. Tsai, and J. C. Kuo, "Real time NURBS Command Generators for CNC Servo Controllers", *International Journal of Machine Tools & Manufacture*, vol. 42, pp.801-813, 2002
- [37] ISO 6983-1 Numeric Control of Machines- Program Format and Definition of Address Words- Part1: Data Format for Positioning, Line Motion, and Contouring Control Systems, 1982
- [38] ISO 14694-1:2003 Industrial Automation Systems and Integration- Physical Device Control- Data Model for Computerized Numerical Controllers- Part 1: Overview and Fundamental Principles, 2003
- [39] Y. Koren, "Computer Control of Manufacturing Systems", McGraw Hill, 1982
- [40] H. Takahashi, and R. J. Bickel, "Developing a Controller to Reduce Contour Error", *Proceedings of 6th International Workshop on Advanced Motion Control*, Nagoya, Japan, pp.222-227, 2000
- [41] Y. Koren, "Cross-coupled Biaxial Computer Control for Manufacturing Systems", *ASME Transaction, Journal of dynamic systems, measurement and control*, vol. 102, no.4, pp.265-272, December 1980
- [42] G. T. Smith, "CNC Machining Technology", Springer-Verlag, 1993
- [43] S. S. Yeh, and M. F. Tu, "A Novel Approach to the Design of NURBS Interpolator for Advanced Motion Systems", *Proceedings of 2005 IEEE International Conference on Mechatronics*, Taipei, Taiwan, pp.388-393, July 2005
- [44] M. C. Tsai, C. W. Cheng, and M. Y. Cheng, "A Real-time NURBS Surface Interpolator for Precision Three-axis CNC machining", *International Journal of Machine Tools & Manufacture*, vol. 43, pp.1217-1227, 2003
- [45] W. T. Lei, M. P. Sung, L. Y. Lin, and J. J. Huang, "Fast Real-time NURBS Path Interpolation for CNC Machine Tools", *International Journal of Machine Tools & Manufacture*, vol. 47, pp.1530-1541, 2007
- [46] D. C. H. Yang, and T. Kong, "Parametric Interpolator versus Linear Interpolator for Precision CNC Machining", *Computer-Aided Design*, vol. 26, no. 3, pp.225-234, 1994
- [47] S. Bedi, I. Ali, and N. Quan, "Advanced Interpolation Techniques for CNC Machines", *ASME Journal of Engineering for Industry*, vol. 115, pp.329-336,

1993

- [48] S. S. Yeh, and P. L. Hsu, "The Speed Controlled Interpolator for Machining Parametric Curves", *Computer-Aided Design*, vol. 31, pp.349-357, 1999
- [49] S. S. Yeh, and P. L. Hsu, "Adaptive-feedrate Interpolation for Parametric Curves with a Confined Chord Error", *Computer- Aided Design*, vol. 34, pp.229-237, 2002
- [50] S. H. Nam, and M. Y. Yang, "A Study on Generalized Parametric Interpolator with Real-time Jerk-limited Acceleration", *Computer-Aided Design*, vol. 36, pp.27-36, 2004
- [51] M. C. Tsai, M. Y. Cheng, K. F. Lin, and N. C. Tsai, "On Acceleration/Deceleration Before Interpolation for CNC Motion Control", *Proceedings of the 2005 IEEE International Conference on Mechatronics*, Taipei, Taiwan, pp.382-387, 2005
- [52] D. I. Kim, J. I. Song, and S. K. Kim, "Dependence of Machining Accuracy on Acceleration/Deceleration and Interpolation Methods in CNC Machine Tools", *IEEE Conference on Industry Applications Society Annual Meeting*, Denver, CO, USA, pp.1898-1905, 1994
- [53] C. W. Cheng, "Design and Implementation of Real-time NURBS Curve and Surface Interpolators for Motion Controllers", *Dissertation for PhD*, National Cheng Kung University, 2003
- [54] D. I. Kim, "Study on Interpolation Algorithms of CNC Machine Tools", *IEEE Conference on Industry Applications Society Annual Meeting*, Orlando, FL, USA, pp.1930-1937,1995
- [55] D. I. Kim, J. W. Jeon, and S. Kim, "Software Acceleration/ Deceleration Methods for Industrial Robots and CNC Machine Tools", *Mechatronics*, vol. 4, no. 1, pp.37-53, 1994
- [56] K. S. Fu, R. C. Gonzalez, and C. S. G. Lee, "Robotics: Control, Sensing, Vision and Intelligence", McGraw Hill, 1987
- [57] DynaCity, "Multi-axis Motion Control & Amplify System DCT0040 User Manual", DynaCity Technology (HK) Ltd., <http://www.dynacitytech.com>